Synthesis and Characterization of Conjugated Mono- and Dithiol Oligomers and Characterization of Their Self-Assembled Monolayers

Bert de Boer,[†,&,#] Hong Meng,[‡,#] Dmitrii F. Perepichka,[‡] Jie Zheng,[§] Martin M. Frank,[∥,⊥] Yves J. Chabal,[∥,⊥] and Zhenan Bao*[,†]

Bell Laboratories, Lucent Technologies, 600 Mountain Avenue, Murray Hill, New Jersey 07974, Department of Chemistry and Biochemistry, University of California at Los Angeles, Los Angeles, California 90095, Department of Chemistry & Biochemistry, Ohio University, Athens, Ohio 45701-2979, Rutgers University, Department of Chemistry and Chemical Biology, Piscataway, New Jersey 08854, and Agere Systems, 600 Mountain Avenue, Murray Hill, New Jersey 07974

Received January 22, 2003. In Final Form: February 25, 2003

The characterization of self-assembled monolayer molecular arrays, which serve as active layers in electronic devices, is an important step toward understanding molecular-scale electronics. To correlate the properties of self-assembled monolayers with their molecular structures, a series of π-conjugated mono- and dithiols and aromatic dithiols with an oxygen or sulfur atom between two aromatic units have been designed and synthesized. Their optical properties were determined by UV−vis spectroscopy. Their self-assembled monolayer films on gold surfaces were characterized by cyclic voltammetry, grazing incidence Fourier transform infrared spectroscopy (GI-FTIR), and contact angle and ellipsometry measurements. Increasing the chain length from two to four phenyl rings showed a more than linear increase of the intensity of the aromatic C═C ring stretch modes in GI-FTIR, indicating that the longer *p*-phenylene system is oriented toward the surface normal. Similar to oligophenylenes, when the number of repeat units for oligothiophene is increased, a more than linear increase of the intensity of the C═C stretch and C−H bend modes implies that the longest oligothiophenedithiol molecule is oriented close to the surface normal. Ellipsometry showed a smaller deviation from the calculated monolayer thickness with increasing number of thiophene or phenylene rings, corroborating the GI-FTIR data. We conclude that the conjugated phenylene- and thiophene-based dithiols demonstrate a less tilted molecular orientation with respect to the surface normal with increasing chain length.

Introduction

With the advent of research activities in nanoscale molecular electronic devices,[1−8] organic thiol compounds have received a great deal of attention in recent years,[9,10] because of their intrinsic semiconductor[11−16] or insulator[17−21] properties. Conjugated thiol-capped compounds such as oligo(1,4-phenylene ethynylene)s and oligo(2,5-thiophene ethynylene)s have been widely studied as molecular wires.[22−29] The broad applications[30] of these

* Corresponding author. Tel: 908-582-4716. Fax: 908-582-4868. E-mail: zbao@lucent.com.
† Lucent Technologies.
‡ University of California at Los Angeles.
§ Ohio University.
∥ Rutgers University.
⊥ Agere Systems.
# These two authors contributed equally to this work.
& Present address: University of Groningen, Materials Science Centre, Department of Physics of Organic Semiconductors, Nijenborgh 4, NL-9747 AG, Groningen, The Netherlands.

(1) Aviram, A.; Ratner, M. A. *Chem. Phys. Lett.* **1974**, *29*, 277.
(2) Goldhaber-Gordon, D.; Montemerlo, M. S.; Love, J. C.; Opiteck, G. J.; Ellenbogen J. C. *Proc. IEEE* **1997**, *85*, 521.
(3) Joachim, C.; Gimzewski, J. K.; Aviram, A. *Nature* **2000**, *408*, 541.
(4) (a) Tans, S. J.; Verschueren, A. R. M.; Dekker, C. *Nature* **1998**, *393*, 49. (b) Postma, H. W. Ch.; Teepen, T.; Yao, Z.; Grifoni, M.; Dekker, C. *Science* **2001**, *293*, 76. (c) Derycke, V.; Martel, R.; Appenzeller, J.; Avouris, Ph. *Nano Lett.* **2001**, *1*, 453. (d) Bachtold, A.; Hadley, P.; Nakanishi, T.; Dekker, C. *Science* **2001**, *294*, 1317.
(5) Martel, R.; Schmidt, T.; Shea, H. R.; Hertel, T.; Avouris, Ph. *Appl. Phys. Lett.* **1998**, *73*, 2447.
(6) Collier, C. P.; Mattersteig, G.; Wong, E. W.; Luo, Y.; Beverly, K.; Sampaio, J.; Raymo, F. M.; Stoddart, J. F.; Heath, J. R. *Science* **2000**, *289*, 1172.
(7) Collier, C. P.; Wong, E. W.; Belohradský, M.; Raymo, F. M.; Stoddart, J. F.; Kuekes, P. J.; Williams, R. S.; Heath, J. R. *Science* **1999**, *285*, 391.
(8) Cui, Y.; Wei, Q.; Park, H.; Lieber, C. M. *Science* **2001**, *293*, 1289.
(9) *Characterization of Organic Thin Films*; Ulman, A., Ed.; Butterworth-Heinemann: Boston, 1995.
(10) Ulman, A. *Chem. Rev.* **1996**, *96*, 1533.
(11) Reed, M. A. *MRS Bull.* **2001**, *26* (2), 113.
(12) Seminario, J. M.; Zacarias, A. G.; Tour, J. M. *J. Am. Chem. Soc.* **1998**, *120*, 3970.
(13) Tour, J. M. *Chem. Rev.* **1996**, *96*, 537.
(14) Borman, S. *Chem. Eng. News* **2001**, *79* (Dec. 10), 45.
(15) Reed, M. A.; Zhou, C.; Muller, C. J.; Burgin, T. P.; Tour, J. M. *Science* **1997**, *278*, 252.
(16) Fan, F. F.; Yang, J.; Dirk, S. M.; Price, D. W.; Kosynkin, D.; Tour, J. M.; Bard, A. J. *J. Am. Chem. Soc.* **2001**, *123*, 2454.
(17) (a) Cui, X. D.; Primak, A.; Zarate, X.; Tomfohr, J.; Sankey, O. F.; Moore, A. L.; Moore, T. A.; Gust, D.; Harris, G.; Lindsay, S. M. *Science* **2001**, *294*, 571. (b) Cui, X. D.; Primak, A.; Zarate, X.; Tomfohr, J.; Sankey, O. F.; Moore, A. L.; Moore, T. A.; Gust, D.; Nagahara, L. A.; Lindsay, S. M. *J. Phys. Chem. B* **2002**, *106*, 8609.
(18) (a) Wold, D. J.; Frisbie, C. D. *J. Am. Chem. Soc.* **2000**, *122*, 2970. (b) Wold, D. J.; Frisbie, D. C. *J. Am. Chem. Soc.* **2001**, *123*, 5549.
(19) Vuillaume, D.; Boulas, C.; Collet, J.; Davidovits, J. V.; Rondelez, F. *Appl. Phys. Lett.* **1996**, *69*, 1646.
(20) Boulas, C.; Davidovits, J. V.; Rondelez, F.; Vuillaume, D. *Phys. Rev. Lett.* **1996**, *76*, 4797.
(21) Mayor, M.; von Hänisch, C.; Weber, H. B.; Reichert, J.; Beckmann, D. *Angew. Chem., Int. Ed.* **2002**, *41*, 1183.
(22) Purcell, S. T.; Garcia, N.; Binh, V. T.; Jones, L., II; Tour, J. M. *J. Am. Chem. Soc.* **1994**, *116*, 11985.
(23) Tour, J. M.; Jones, L., II; Pearson, D. L.; Lamba, J. J. S.; Burgin, T. P.; Whitesides, G. M.; Allara, D. L.; Parikh, A. N.; Atre, S. V. *J. Am. Chem. Soc.* **1995**, *117*, 9529.
(24) Donhauser, Z. J.; Mantooth, B. A.; Kelly, K. F.; Bumm, L. A.; Monnell, J. D.; Stapleton, J. J.; Price, D. W., Jr.; Rawlett, A. M.; Allara, D. L.; Tour, J. M.; Weiss, P. S. *Science* **2001**, *292*, 2303.
(25) Yaliraki, S. N.; Kemp, M.; Ratner, M. A. *J. Am. Chem. Soc.* **1999**, *121*, 3428.

10.1021/la0341052 CCC: $25.00
Published on Web 03/29/2003

Scheme 1. Synthesis of Aromatic Dithiols via Chlorosulfonation[a]

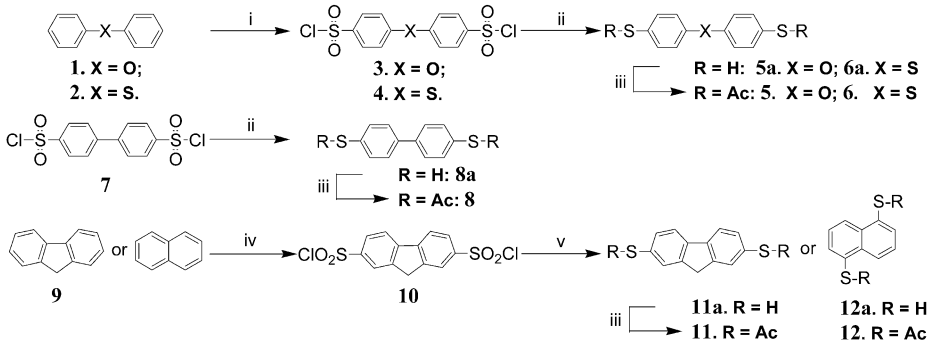

[a] Reagents: (i) $ClSO_3H$. (ii) 1. Zn/Hg; 2. H_2SO_4. (iii) $AcCl/Et_3N$. (iv) 1. $ClSO_3H$/AcOH; 2. PCl_5. (v) $SnCl_2$/HCl.

conjugated thiol compounds in molecular electronics are results of their unique capability to form well-ordered monolayers via the self-assembly process onto gold or other metal surfaces.[9,10,31−36] This provides a convenient method for surface modification as well as deposition of active materials for various thin film device applications. The scanning tunneling microscopy (STM) observation of high molecular order in conjugated arylthiol self-assembled monolayers (SAMs) indicates the feasibility of using conjugated thiols in electronic devices.[24,26,27,33,37,38] The past few years have also witnessed conjugated thiols being widely used in different areas ranging from modification of electrodes[39−42] and sensor devices[43] to the field of molecular electronics, for example, molecular switches,[24,44] random access memory cells,[45] rectifiers,[46,47] and transistors.[48,49] Although extensive research work has been done on the characterization of alkanethiol SAMs, reports on the synthesis and characterization of SAMs of conjugated thiols are limited.[13,23,50−53] These rigid conjugated thiols with tunable electronic properties are attractive candidates for molecular electronic devices.[23,43−49] In this paper, we report the synthesis of various conjugated mono- and dithiol oligomers in order to understand the effect of molecular structure on self-assembled monolayer formation. Four types of synthetic strategies were used, depending on the target molecules. The optical band gap of the molecules was determined by UV−vis spectroscopy. The self-assembled monolayers were characterized by grazing incidence Fourier transform infrared spectroscopy (GI-FTIR), contact angle measurements, ellipsometry, and cyclic voltammetry. The detailed results of this characterization, together with the synthetic strategies, are presented in this paper.

Results and Discussion

Synthesis. A wide variety of aromatic and heteroaromatic thiols were synthesized to understand the structure−property relationships. Since aromatic dithiol compounds are usually easily oxidized and likely to polymerize through disulfide formation and, therefore, are difficult to handle, we used acetyl protection for the thiol functional groups similar to those described by Tour et al.[13,23,52]

Four general strategies have been used to synthesize various conjugated thiols: direct chlorosulfonation followed by reduction (Scheme 1), sulfurization of organometallic compounds (Scheme 2), coupling of acetyl-protected thiols (Scheme 3), and coupling of methyl-protected thiols and subsequent demethylation (Schemes 4 and 5). Direct chlorosulfonation followed by reduction is an effective method to synthesize aromatic mono- and dithiols.[54] The arylsulfonyl chlorides were reduced with either zinc dust amalgam[55,56] or stannous chloride in glacial acetic acid saturated with hydrogen chloride.[56] Direct chlorosulfonation is particularly useful for the synthesis of electron-rich phenylthiol derivatives such as biphenyl, fluorene, and 1,5-naphthalenedithiols (Scheme 1).

(26) Cygan, M. T.; Dunbar, T. D.; Arnold, J. J.; Bumm, L. A.; Shedlock, N. F.; Burgin, T. P.; Jones, L., II; Allara, D. L.; Tour, J. M.; Weiss, P. S. *J. Am. Chem. Soc.* **1998**, *120*, 2721.
(27) Lin, P.-G.; Guyot-Sionnest, P. *Langmuir* **1999**, *15*, 6825.
(28) Zehner, R. W.; Sita, L. R. *Langmuir* **1997**, *13*, 2973.
(29) Reichert, J.; Ochs, R.; Beckmann, D.; Weber, H. B.; Mayor, M.; v. Löhneysen, H. *Phys. Rev. Lett.* **2002**, *88*, 176804-1.
(30) Fendler, J. H. *Chem. Mater.* **2001**, *13*, 3196.
(31) Nuzzo, R. G.; Allara, D. L. *J. Am. Chem. Soc.* **1983**, *105*, 4481.
(32) Finklea, H. O. *Electroanal. Chem.* **1996**, *19*, 109.
(33) Dunbar, T. D.; Cygan, M. T.; Bumm, L. A.; McCarty, G. S.; Burgin, T. P.; Reinerth, W. A.; Jones, L., II; Jackiw, J. J.; Tour, J. M.; Weiss, P. S.; Allara, D. L. *J. Phys. Chem. B* **2000**, *104*, 4880.
(34) Laibinis, P. E.; Whitesides, G. M.; Allara, D. L.; Tao, Y.-T., Parikh, A. N.; Nuzzo, R. G. *J. Am. Chem. Soc.* **1991**, *113*, 7152.
(35) Walczak, M. M.; Chung, C.; Stole, S. M.; Widrig, C. A.; Porter, M. D. *J. Am. Chem. Soc.* **1991**, *113*, 2370.
(36) (a) Twardowski, M.; Nuzzo, R. G. *Langmuir* **2002**, *18*, 5529. (b) Kumar, A.; Abbott, N. L.; Biebuyck, H. A.; Kim, E.; Whitesides, G. M. *Acc. Chem. Res.* **1995**, *28*, 219.
(37) Hong, S.; Reifenberger, R.; Tian, W.; Datta, S.; Henderson, J.; Kubiak, C. P. *Superlattices Microstruct.* **2000**, *28*, 289.
(38) Dhirani, A.; Zehner, R. W.; Hsung, R. P.; Guyot-Sionnest, P.; Sita, L. R. *J. Am. Chem. Soc.* **1996**, *118*, 3319.
(39) Dudek, S. P.; Sikes, H. D.; Chidsey, C. E. D. *J. Am. Chem. Soc.* **2001**, *123*, 8033.
(40) Zhu, L.; Tang, H.; Harima, Y.; Yamashita, K.; Hirayama, D.; Aso, Y.; Otsubo, T. *Chem. Commun.* **2001**, 1830.
(41) Campbell, I. H.; Kress, J. D.; Martin, R. L.; Smith, D. L.; Barashkov, N. N.; Ferraris, J. P. *Appl. Phys. Lett.* **1997**, *71*, 3528.
(42) Zehner, R. W.; Parsons, B. F.; Hsung, R. P.; Sita, L. R. *Langmuir* **1999**, *15*, 1121.
(43) Hutchison, J. E.; Postlethwaite, T. A.; Murray, R. W. *Langmuir* **1993**, *9*, 3277.
(44) (a) Chen, J.; Reed, M. A.; Rawlett, A. M.; Tour, J. M. *Science* **1999**, *286*, 1550. (b) Chen, J.; Wang, W.; Reed, M. A.; Rawlett, A. M.; Price, D. W.; Tour, J. M. *Appl. Phys. Lett.* **2000**, *77*, 1224.
(45) Reed, M. A.; Chen, J.; Rawlett, A. M.; Price, D. W.; Tour, J. M. *Appl. Phys. Lett.* **2001**, *78*, 3735.
(46) Metzger, R. M. *Acc. Chem. Res.* **1999**, *32*, 950.
(47) Dhirani, A.; Lin, P.-H.; Guyot-Sionnest, P.; Zehner, R. W.; Sita, L. R. *J. Chem. Phys.* **1997**, *106*, 5249.
(48) Park, J.; Pasupathy, A. N.; Goldsmith, J. I.; Chang, C.; Yaish, Y.; Petta, J. R.; Rinkoski, M.; Sethna, J. P.; Abruña, H. D.; McEuen, P. L.; Ralph, D. C. *Nature* **2002**, *417*, 722.
(49) Liang, W.; Shores, M. P.; Bockrath, M.; Long, J. R.; Park, H. *Nature* **2002**, *417*, 725.
(50) Hsung, R. P.; Babcock, J. R.; Chidsey, C. E. D.; Sita, L. R. *Tetrahedron Lett.* **1995**, *36*, 4525.
(51) Sabatani, E.; Cohen-Boulakia, J.; Bruening, M.; Rubinstein, I. *Langmuir* **1993**, *9*, 2974.
(52) Tour, J. M. *Acc. Chem. Res.* **2000**, *33*, 791.
(53) Hicks, R. G.; Nodwell, M. B. *J. Am. Chem. Soc.* **2000**, *122*, 6746.
(54) Suter, C. M. *J. Am. Chem. Soc.* **1931**, *53*, 1112.
(55) Caesar, P. D. *Org. Synth. Coll. Vol. IV* **1963**, 695.
(56) Marvel, C. S.; Caesar, P. D. *J. Am. Chem. Soc.* **1951**, *73*, 1097.

Scheme 2. Formation of Aromatic Dithiols by Sulfurization of Organometallic Compounds[a]

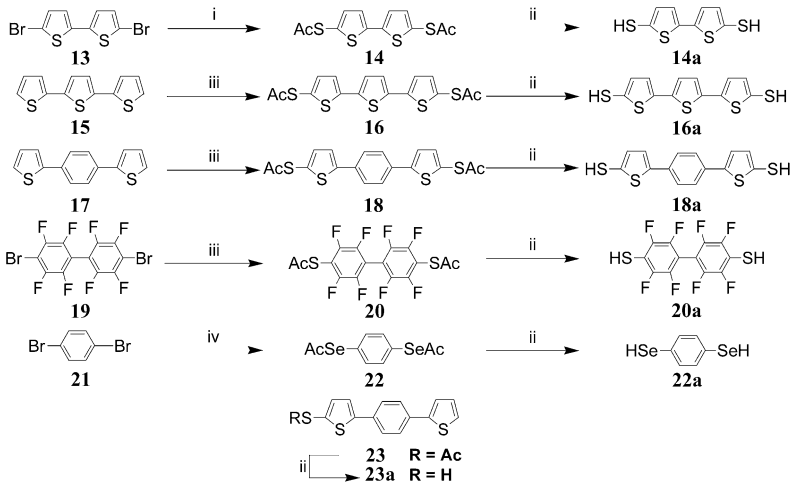

[a] Reagents: (i) 1. Mg/THF; 2. S; 3. AcCl. (ii) NH_4OH. (iii) 1. *n*-BuLi/THF; 2. S; 3. AcCl. (iv) 1. *t*-BuLi; 2. Se; 3. AcCl.

Scheme 3. Synthesis of Diphenylacetylenedithiol[a]

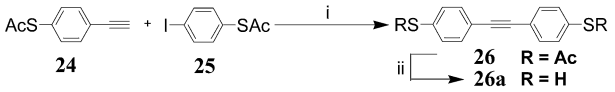

[a] Reagents: (i) 1. *N*,*N*-*i*-Pr_2EtN/THF; 2. $Pd(PPh_3)_2Cl_2$/CuI, 50 °C, 24 h. (ii) NH_4OH.

Scheme 4. Synthesis of Methyl Thioethers of Oligophenylene and Oligophenylenethiophene Derivatives by the Suzuki Coupling Reaction[a]

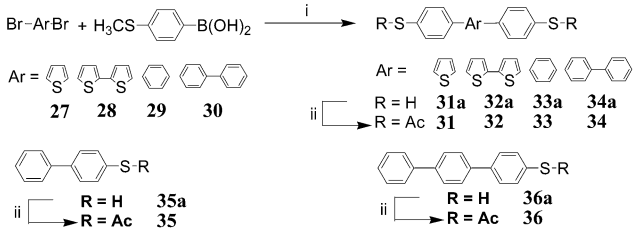

[a] Reagents: (i) 1. $Pd(PPh_3)_4/Na_2CO_3$; 2. *t*-BuSNa. (ii) AcCl/Et_3N.

Scheme 5. Synthesis of Quaterthiophenedithiol[a]

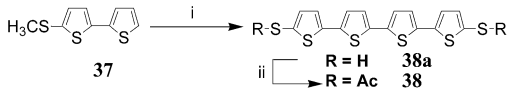

[a] Reagents: (i) 1. *n*-BuLi, CuCl; 2. *t*-BuSNa. (ii) AcCl/Et_3N.

Incorporation of heteroatoms (N, O, S, Se) in phenyl-based systems has been shown to transmit electronic effects efficiently.[57,58] Therefore, the dithiol derivatives of phenyl ether **5a** and phenylthioether **6a** were synthesized (Scheme 1). Arylsulfonyl chlorides **3** and **4**, prepared by direct chlorosulfonation of phenyl (thio)ether, were reduced with zinc dust amalgam to give dithiols **5a** and **6a**, respectively, which were protected by acylation.[55,56] Since the biphenyl moiety (**8a**) is twisted in solution, which affects the conjugation, a planar fluorene homologue **11a** was therefore synthesized (Scheme 1). Reduction of the sulfonyl chloride in this case has been performed with stannous chloride in HCl-saturated acetic acid.[56] This method was found to be particularly useful for those less soluble aryldithiols with higher melting points (such as 1,5-naphthalenedithiols **12a**).

Aromatic Grignard reagents and lithium compounds can react with sulfur, followed by acetylation, to give aromatic thioacetyl derivatives (Scheme 2).[23,59] This method is most useful for thiophene-containing oligomers (such as compounds **15** and **17**) and aromatic halides (such as compounds **13** and **19**). However, an excess of organometallic compound with respect to sulfur is essential to prevent the formation of disulfides. Octafluoro derivative **20** was synthesized as an electron acceptor analogue of biphenyldithiol (Scheme 2). Controlling the stoichiometry of the above reaction (Scheme 2) afforded an analogous monothiol derivative of 1,4-dithienylbenzene (**23a**).

Different coupling reactions were employed to synthesize longer oligomeric aromatic cores (Schemes 3−5).[50,59−62] In this case, the thiol group has to be protected to avoid side reactions. Acetyl-protected thiols are found to work well for the coupling reactions between phenylacetylene and aryl halides. This method has been used by Tour's group to synthesize molecular wires as long as 128 Å.[61,62] Accordingly, diphenylacetylene **26** was prepared in a one-step cross-coupling reaction (Scheme 3) to study the influence of the acetylene linker.

For other types of coupling reactions, methyl-protected thiols were found to give higher yields of the products that can be deprotected almost quantitatively using the recently reported method of Gingras and co-workers.[63] Thus, Suzuki coupling of 4-(methylthio)phenylboronic acid with different dibromothiophene and dibromophenyl homologues gave phenylene-thiophene and oligophenylene derivatives, respectively. They were demethylated with sodium *tert*-butylthiolate and subsequently protected with acetyl groups to give the target dithioacetyl derivatives **31**−**36** (Scheme 4). Similarly, 4-mercaptobiphenyl (**35a**) and 4-mercaptoterphenyl (**36a**) were synthesized by a Suzuki coupling of 4-(methylthio)phenylboronic acid with bromobenzene and 4-bromobiphenyl, respectively.

(57) Di Ventra, M.; Lang, N. D. *Phys. Rev. B* **2001**, *65*, 045402-1.
(58) (a) Kobayashi, E.; Metaka, N.; Aoshima, S.; Furukawa, J. *J. Polym. Sci., Part A: Polym. Chem.* **1992**, *30*, 227. (b) Litvinenko, L. M.; Cheshko, R. S. *J. Gen. Chem. USSR* **1960**, *30*, 3682. (c) Litvinenko, L. M.; Popova, R. S.; Popov, A. F. *Russ. Chem. Rev.* **1975**, *44*, 718.
(59) (a) Houff, W. M.; Schuetz, R. D. *J. Am. Chem. Soc.* **1953**, *75*, 6316. (b) Jones, E.; Moodie, I. M. *Org. Synth.* **1970**, *50*, 104. (c) Adams, R.; Ferretti, A. *J. Am. Chem. Soc.* **1959**, *81*, 4939.
(60) Rane, A. M.; Miranda, E. I.; Soderquist, J. A. *Tetrahedron Lett.* **1994**, *35*, 3225.
(61) Jones, L., II; Schumm, J. S.; Tour, J. M. *J. Org. Chem.* **1997**, *62*, 1388.
(62) Pearson, D. L.; Tour, J. M. *J. Org. Chem.* **1997**, *62*, 1376.
(63) Pinchart, A.; Dallaire, C.; Van Bierbeek, A.; Gingras, M. *Tetrahedron Lett.* **1999**, *40*, 5479.

Table 1. UV−Vis Absorption Maxima, Optical Band Gaps, and Oxidation Potentials of Conjugated Mono- and Dithiols

molecule	λ_{max} (nm)[a]	E_g (eV)[b]/nm	E_{ox}^{pa}/E_{ox}^{pc} (V)[c]
1,4-benzenedithiol	261	3.80/326	
5	252	4.13/300	+1.42/×[d]
6	265	3.82/325	+1.48/×
8	290	3.85/322	+1.53/×
11	312	3.82/325	+1.33/×
12	301	3.82/325	+1.49/×
14	338	3.18/390	+1.31/×
16	380	2.82/440	+0.98/+0.90
18	349	3.18/390	+1.03/+0.97
20	265	4.00/310	×/×
22	274	3.79/327	×/×
23	340	3.24/383	+1.48/×
26	321	3.44/360	+1.50/×
31	345	3.18/390	+1.50/×
32	390	2.95/420	+1.02/×
33	304	3.54/350	+1.38/×
34	318	3.44/360	+1.42/×
35	267	3.97/312	+1.52/×
36	291	3.66/339	+1.35/×
38	412	2.64/470	+0.81/+0.67

[a] The maximum of the longest wavelength absorption (λ_{max}) in THF. [b] E_g = optical band gap in eV (and nm) determined as the onset of the absorption spectrum at the red-edge. [c] Potentials of the anodic and cathodic peaks (when observed) of the electrochemical oxidation wave, vs Ag/Ag^+; scan rate, 50 mV s^{-1}. [d] × = Peak not observed.

A Cu(I)-catalyzed coupling reaction of 5-methylthio-2,2′-bithiophene-5′-lithium followed by the above-mentioned demethylation−acetylation sequence yielded compound **38** with a quaterthiophene aromatic core (Scheme 5).

Self-Assembled Monolayer Formation. The self-assembly of alkanethiols is usually carried out under relatively high concentrations (1−10 mM). However, the self-assembly of conjugated mono- or dithiols has to be performed in much more dilute solutions (≪1 mM) to avoid multilayer formation (see below) and precipitation due to poor solubility of some conjugated thiols. In addition, conjugated thiols can easily dimerize due to oxidative disulfide formation. Therefore, in situ deprotection of thioacetyl groups by addition of NH_4OH was used to generate free thiols in nearly quantitative yield.[23] Acetyl-protected monothiols completely suppress dimerization and form good-quality SAMs. For dithiols, however, Tour and co-workers[23] showed that the problem still existed for self-assembly conducted at high concentrations, even when the protection approach was utilized (presumably due to the reaction with residual traces of oxygen). It was also observed that direct adsorption of the deprotected dithiols appeared to be an excellent method to prevent multilayer formation.[23] Weiss and co-workers have found that self-assembly performed under reflux conditions gives much larger domains of well-ordered SAMs.[64]

Absorption Spectra. The UV−vis spectra of the mono- and dithiol oligomers were recorded in tetrahydrofuran (THF) solution using 10 × 10 mm quartz cells and a spectral range of 200−700 nm. The lowest energy UV−vis absorption peaks (λ_{max}) of the studied aromatic acetyl-protected thiols are listed in Table 1. The absorption bands were practically unchanged after deprotection. For deprotected ter- and quaterthiophenes **16** and **38**, however, additional lower energy bands (459 and 490 nm, respectively) were observed as a result of oxidation of the highly air-sensitive oligothiophene dithiols (the intensity of this band can be drastically diminished by thorough degassing of the solution before deprotection). Introducing the (thio)-ether (**5** and **6**) linkage between two phenyl rings clearly interrupts the π-conjugation of **8** as witnessed by a blue shift of the absorption maximum. The thioether (**6**) showed a lower energy absorption band (higher λ_{max}) compared to the ether (**5**). Predictably, the thioacetyl groups result in a red shift of the absorption maxima and lower the optical band gap (E_g), which is demonstrated by comparing monosubstituted compounds **23** and **36** with disubstituted **18** and **33**, respectively. Selenoacetyl groups (**22**) only slightly affect the optical properties, compared to the thiogroup (1,4-benzenedithiol). Introducing a rigid bridge between two phenyl rings (fluorene **11** vs biphenyl **8**) forces both rings to be planar and increases the π-orbital overlap. The nonplanarity of oligo(*p*-phenylene)s, with a torsion angle between two rings of ∼45−50° (in solution) due to intramolecular repulsion of the ortho hydrogens,[65] results in only a relatively small increase of the absorption maxima (λ_{max}) with the chain length (**8**, **33**, and **34**) compared to their thiophene analogues (**14**, **16**, and **38**) (more planar conformation in solution). In the solid state, however, the intermolecular packing interactions may overcome the intramolecular steric repulsion in oligo(*p*-phenylenes) and force the rings to coplanarity.[66]

Cyclic Voltammetry. The electrochemistry of redox active SAMs has attracted broad attention for the past decade.[67−69] Besides being an invaluable tool in studying SAMs, it was used in SAM-based sensing devices[69b,c] as well as for chemical modification of self-assembled molecules.[67] The electrochemical behavior of the studied aromatic thioacetyl derivatives in solution is represented by a multielectron irreversible or partially quasi-reversible oxidation wave (Table 1), which splits into two unresolved waves in some cases. As expected, the oxidation potential depends strongly on the nature of the conjugated core: incorporation of electron-rich thiophene units facilitates the oxidation process; the lowest oxidation potential was found for quaterthiophene **38a**. Extension of the π-conjugation by introducing *p*-phenylene units also substantially decreases the E_{ox} values (cf. **18** or **32** vs **14**), but in the case of the pure oligophenylene backbone (**8** → **33** → **34**) this tendency is not so pronounced, as a result of poor conjugation in oligophenylenes due to significant twisting of benzene rings. Figure 1 shows the cyclic voltammetric behavior of terthiophene **16** (in solution) and SAM **16a**. In both cases, scanning into positive potentials resulted in a partially reversible oxidation wave whose position is sensitive to the scan rate. The chemical reversibility (i.e., cathodic to anodic peak current ratio) increased at higher scan rates, indicating that a slow irreversible chemical reaction follows the oxidation. Multiple scanning of the SAM between 0 and 1.35 V resulted in disappearance of the oxidation wave. The irreversibility of radical cation formation is a common feature of short oligothiophenes, even though some derivatives (e.g., **39**) can give a very stable radical cation.[53] In the case of **39**, oxidation occurs as two single electron waves at E_{ox}^0 = 0.86 and 1.02 V versus saturated calomel electrode (SCE), respectively (ca.

(64) Bumm, L. A.; Arnold, J. J.; Charles, L. F.; Dunbar, T. D.; Allara, D. L.; Weiss, P. S. *J. Am. Chem. Soc.* **1999**, *121*, 8017.

(65) *Handbook of Organic Conductive Molecules and Polymers*; Nalwa, H. S., Ed.; John Wiley & Sons: New York, 1997; Vols 1−4.

(66) Socci, E. P.; Farmer, B. L.; Baker, K. N. *Polymer* **1993**, *34*, 1571.

(67) Kwan, W. S. V.; Atanasoska, L.; Miller, L. L. *Langmuir* **1991**, *7*, 1419.

(68) Berlin, A.; Zotti, G. *Macromol. Rapid Commun.* **2000**, *21*, 301 and references therein.

(69) (a) Fujihara, H.; Nakai, H.; Yoshihara, M.; Maeshima, T. *Chem. Commun.* **1999**, 737. (b) Liu, H.; Liu, S.; Echegoyen, L. *Chem. Commun.* **1999**, 1493. (c) Liu, S.; Liu, H.; Bandyopadhyay, K.; Gao, Z.; Echegoyen, L. *J. Org. Chem.* **2000**, *65*, 3292.

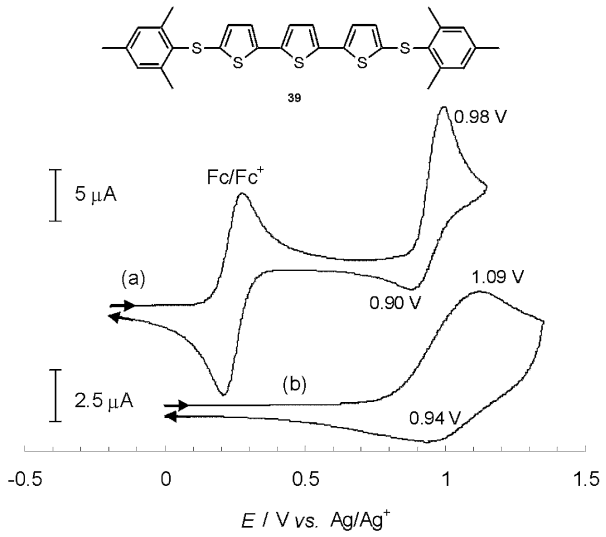

Figure 1. Cyclic voltammograms of (a) compound **16** in solution and (b) deprotected dithiol **16a** as a SAM on a Au electrode (ref 71); scan rate, 50 mV s^{-1}.

0.66 and 0.82 V vs Ag/Ag^+). These low potentials and a small gap between the first and the second oxidation wave for **39** suggest that the oxidation wave observed for **16** at +0.98 V versus Ag/Ag^+ is actually a two-electron process; indeed, preliminary experiments show its splitting into two waves at lower temperature.[70] The detailed study of the electrochemistry of SAMs of this and other oligothiophene derivatives is under way.

Grazing Incidence FTIR and Ellipsometry. Ever since the discovery of SAMs of alkanethiolates absorbed on metal surfaces,[31] GI-FTIR has been used as a powerful technique to determine the orientation of aliphatic molecules tethered to the surface.[9,72] With GI-FTIR on metal substrates (or any near-perfect conductor at IR frequencies), the component of the external electric field (IR light) parallel to the surface plane is almost completely screened by the electronic polarization of the metal. Therefore, the measured infrared band intensity of a vibrational mode directly depends on the projection of its transition dipole moment onto the surface normal. This implies that one can only probe IR modes that have a nonzero component of the transition moment along the surface normal, that is, perpendicular to the gold surface.[72] With the increasing interest in self-assembled monolayers of conjugated (or semiconducting) thiols on gold substrates for molecular electronics, a detailed picture of the orientation of conjugated thiols with respect to the gold surface is required. The combination of GI-FTIR and ellipsometry can provide information on the intrinsic structure of the SAMs and provide a better understanding of those monolayers (and eventually of device performance). We found that the SAM film thicknesses measured by ellipsometry are in good agreement with the calculated molecular lengths. This, together with the GI-FTIR results discussed below, is a good indication that only one monolayer of mono- or dithiol molecules was deposited with the long molecular axis pointing along the gold surface normal (edge-on on the gold surface) (Table 3). The average film thickness, measured at different spots of the same film (as large as 10 cm^2), differs only by a few angstroms. The difference between the measured and calculated thicknesses might be a result of a small tilt with respect to the surface normal of the molecules in the monolayer or the average value used for the refractive index of the SAM in calculating the layer thickness from the measured psi (ψ) and delta (δ) values (1.55 and 1.45 for all the conjugated thiols[73] and hexadecanethiol,[35] respectively).

All the vibrational bands observed in the GI-FTIR spectra of oligothiophene SAMs are assigned according to ref 74. For the SAMs of compounds **18a**, **23a**, **31a**, and **32a** on gold, a combination of vibrational modes found in oligophenylenes (**8a**, **33a**, and **34a**) and oligothiophenes (**14a** and **16a**) is invoked, as described below. In all the spectra taken on compounds containing thiophene rings, broad peaks are present at 1170−1180 cm^{-1} and around 1330 cm^{-1} and are assigned to an oxidized sulfur species, probably a sulfone. The intensity of the ~1175 cm^{-1} peak increases upon exposure to air. A similar broad peak has also been reported for phenyleneethynylene-based thiols and was assigned to the S=O stretching of sulfone.[23] Furthermore, one can infer from the GI-FTIR spectra that the deprotection of the thioacetyl moiety is not quantitative for most phenyl-based compounds. Indeed, a relatively small amount of grafted molecules still possess a thioacetyl group, as evidenced by a band just above 1700 cm^{-1} that is assigned to a strong C=O stretching mode of the thioacetyl group.

Figure 2 illustrates the dependence of the component of the transition dipole moment along the surface normal on the orientation of the rigid conjugated thiol. The transition dipole moments are expressed with respect to the molecular coordinate system with *L* denoting a transition dipole moment oriented along the molecular axis, *M* a transition dipole moment in the plane of the molecule and perpendicular to *L*, and *N* a transition dipole moment perpendicular to the molecular plane. In Figure 2A−C, different orientations of the rigid molecule are depicted with the out-of-plane mode *N* parallel to the gold surface (not IR active). Figure 2D illustrates a general dependence of the normal components of *L*, *M*, and *N* on the tilt angle (α) and the rotation angle (β). Figure 2C,E,F illustrates the special cases where the molecule axis is parallel ($\alpha = 90°$) to the gold surface ($L = 0$) and $\beta = 0°$ (Figure 2F, $N = 1$) and 90° (Figure 2C, $M = 1$).

In GI-FTIR, one can clearly distinguish components of the stretching and bending modes that are perpendicular to the gold surface (Table 2). Spectra of SAMs of phenylene-based (Figure 3) and thiophene-based dithiols on gold (Figure 4) are given as typical examples. The spectra from phenylene-based dithiols (Figure 3) exhibit strong absorption signals due to the aromatic C=C ring stretch mode (~1475 cm^{-1}, mostly oriented along *L*, with a smaller component along M) and the aromatic C−H stretch modes of phenyl rings (~3030 cm^{-1}, components in *M* and *L*),

(70) Exhaustive electrolysis (at the potential of the anodic peak) of **16** consumes four to six electrons per molecule (depending on the electrolysis conditions), suggesting that not only the terthiophene core but also the side thiol groups are subject to oxidation. However, this value is not in direct connection with the kinetically controlled CV experiment, due to the irreversible nature of the process.

(71) Integration of the anodic peak area gives (ref 31) the estimated surface coverage of $\approx 2 \times 10^{-9}$ mol cm^{-2}, which corresponds to a molecular area of ca. 35 $Å^2$, calculating for the two-electron process.

(72) Parikh, A. N.; Allara, D. L. *J. Chem. Phys.* **1992**, *96*, 927.

(73) An isotropic refractive index is used to calculate the film thickness even though the refractive index is expected to be highly anisotropic for these SAMs, implying that the film thicknesses measured are relative thicknesses. Therefore, absolute tilt angles were not calculated from these data. The ellipsometric data support the formation of a single monolayer instead of multilayers. Recalculating the layer thicknesses with a (isotropic) refractive index of 1.45 gave rise to a ~10% increase of the measured layer thickness.

(74) (a) Liedberg, B.; Yang, Z.; Engquist, I.; Wirde, M.; Gelius, U.; Götz, G.; Bäuerle, P.; Rummel, R.-M.; Ziegler, Ch.; Göpel, W. *J. Phys. Chem. B* **1997**, *101*, 5951. (b) Louarn, G.; Buisson, J. P.; Lefrant, S.; Fichou, D. *J. Phys. Chem.* **1995**, *99*, 11399.

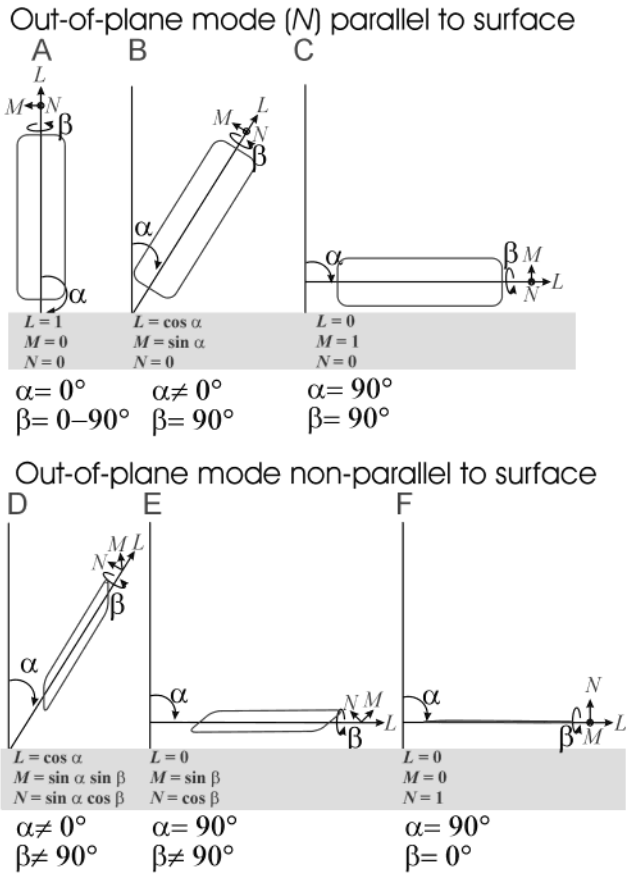

Figure 2. Schematic illustration of various vibrational transition dipole moments (*L*, *M*, and *N*) and the dependence of their component along the surface normal (determining their IR activity) on molecular orientation. *L*, *M*, and *N* denote modes oriented along the chain axis and in-plane and out-of-plane modes oriented normal to the chain axis, respectively.

which implies that the phenylene-based compounds are oriented away from the gold surface (excluding the orientations in Figure 2C,E,F). The nonlinear increase of the intensity of the C=C aromatic ring stretch mode with the number of phenyl rings (**8a** at 1475 cm^{-1}, **33a** at 1479 cm^{-1}, and **34a** at 1479 cm^{-1}) shows that the tilt angle (α) decreases in the same order. Furthermore, a shift of this peak (~1475 cm^{-1}) toward lower frequency would be expected for phenylenes with the long axis (*L*) tilted toward the gold surface.[75] As this peak is shifted to higher frequency, we conclude, in combination with the nonlinear increase in the intensity of this peak, that the longer *p*-phenylene systems (**33a** and **34a**) have a smaller tilt angle (α) than **8a**.[75,76] Since the out-of-plane modes at ~815 cm^{-1} are nonzero for the phenyl-based dithiols, we can exclude the orientation depicted in Figure 2A−C in favor of the orientation depicted in Figure 2D. The intensity of the out-of-plane mode at ~815 cm^{-1} depends on the tilt angle α and the rotation angle β. The dependence of the out-of-plane modes on β is often neglected but might have a substantial influence on this mode. This can be simply visualized by considering Figure 2B with $\beta = 90°$ (no out-of-plane mode is IR active and no dependence on α) and $\beta = 0°$ (*N* depends solely on sin α). Since some oligophenylenes crystallize in a herringbone arrangement, as also proposed for SAMs of terphenylenes,[77] and other oligophenylenes favor $\pi-\pi$ stacking, the average value of β may vary from system to system. Leung and co-workers showed that two different phases coexist for 4-methyl-4′-mercaptobiphenyl on gold: the striped phase with a tilt angle at least 15° from the surface normal and the hexagonal phase purely consisting of $(\sqrt{3}\times\sqrt{3})$R30° structure.[78] Very likely, this is also true for our 4,4′-dimercaptobiphenyl SAM on gold.

Research previously conducted on terphenylmonothiol **36a** SAMs revealed that the observed phases depend on the solvent used.[51,76,79−81] Furthermore, it was proposed that phenyl-, biphenyl- (**35a**), and terphenylmonothiols (**36a**) can adopt two different orientations on a gold surface, namely, sp and sp^3, where sp implies a straight bond Au−S−C (180°) and sp^3 refers to an angle of ~120° for Au−S−C.[79,82] The orientation clearly depends on the solvent used, suggesting that the solvent−molecule−substrate interactions and the decrease in entropy have to compete with $\pi-\pi$ stacking interactions and the decrease in surface tension due to the sulfur−gold bond. The competition between two orientations results in a less ordered monolayer for terphenylmonothiol. Our measurements show that biphenylmonothiol (**35a**) and terphenylmonothiol (**36a**) assemble with their out-of-plane C−H bend modes (oriented along *N*) parallel to the surface as witnessed by the complete disappearance of the out-of-plane C−H bend mode located at ~815 cm^{-1}, consistent with previous data from terphenylthiol.[77] This does not imply that the monothiols are oriented along the surface normal since relatively strong C−H vibration modes are still observed for **35a** and **36a**. The strong C−H vibration modes (along molecular coordinates *M* and *L*) and the disappearance of the out-of-plane C−H mode (along *N*) can only be explained by taking into account a small tilt angle (α) and a rotation angle (β) of 90° (Figure 2B). Though the monothiols described above have a substantial dipole moment along the asymmetric phenyl chain, which can influence the packing when grafted on the gold surface, the class of dithiols used here are initially symmetric and thus have a very small dipole once grafted on the gold surface. Consequently, the more favorable interchain interaction will influence the packing on the gold surface similar to biphenyl systems with a small molecular dipole moment.[83] The GI-FTIR data combined with the data obtained from ellipsometry (Table 3) suggest that increasing the number of phenyl rings forces the molecules to align vertically on the surface as observed previously in similar systems.[76,77]

Both the symmetric and asymmetric C−H stretch modes of the CH_2 bridge (~2930 cm^{-1}) of the fluorenedithiol (**11a**) SAM are not observed by GI-FTIR, implying that the CH_2 planes are oriented parallel to the gold surface. Ellipsometry measurements also suggest that the fluorenedithiol layer thickness corresponds to the fully extended fluorene molecule oriented nearly along the surface normal. The other modes that are also seen in **8a** are clearly identified (Table 2).

(75) Brower, T. L.; Garno, J. C.; Ulman, A.; Liu, G.-Y.; Yan, C.; Gölzhäuser, A.; Grunze, M. *Langmuir* **2002**, *18*, 6207.
(76) Frey, S.; Stadler, V.; Heister, K.; Eck, W.; Zharnikov, M.; Grunze, M.; Zeysing, B.; Terfort, A. *Langmuir* **2001**, *17*, 2408.
(77) (a) Fuxen, C.; Azzam, W.; Arnold, R.; Witte, G.; Terfort, A.; Wöll, C. *Langmuir* **2001**, *17*, 3689. (b) Azzam, W.; Wehner, B. I.; Fisher, R. A.; Terfort, A.; Wöll, C. *Langmuir* **2002**, *18*, 7766.
(78) Leung, T. Y. B.; Schwartz, P.; Scoles, G.; Schreiber, F.; Ulman, A. *Surf. Sci.* **2000**, *458*, 34.
(79) Ishida, T.; Mizutani, W.; Azehara, H.; Sato, F.; Choi, N.; Akiba, U.; Fujihira, M.; Tokumoto, H. *Langmuir* **2001**, *17*, 7459.
(80) Ishida, T.; Mizutani, W.; Choi, N.; Akiba, U.; Fujihira, M.; Tokumoto, H. *J. Phys. Chem. B* **2000**, *104*, 11680.
(81) Chang, S.-C.; Chao, I.; Tao, Y.-T. *J. Am. Chem. Soc.* **1994**, *116*, 6792.
(82) Tao, Y.-T.; Wu, C.-C.; Eu, J.-Y.; Lin, W.-L. *Langmuir* **1997**, *13*, 4018.
(83) Ulman, A. *Acc. Chem. Res.* **2001**, *34*, 855.

Table 2. Overview and Assignments of the Modes Probed by GI-FTIR

	GI-FTIR (cm^{-1})									
compound[a]	C−H wag	ring stretch + bend	arom C−C ring stretch[b]	C−H bend[b]	C−O(S)−C stretch	C−H rock	ΣC−H wag	arom C−H stretch	CH_2 stretch[b]	CH_3 stretch[b]
$C_{16}H_{33}SH$[c]				1468 (sc)					2920 (a), 2851 (s)	2964 (a), 2878 (s)
22a		957, 1161, 1252	1005 (i), 1375, 1516	849		1670	1749, 1869	3095		
HS−C_6H_4−SH	783	957, 1173, 1254	1007 (i), 1362, 1468	847		1566, 1670	1759	3093		
8a[d]	714	1045, 1132, 1200	1001 (i), 1475 (s)[g]	814 (o)		1593, 1659	1755			
33a	729	1057, 1142, 1188	1001 (i), 1394, 1479 (s)[g]	810 (o)		1591	1913	3032, 3057		
34a	721	1122, 1182, 1255	1001 (i), 1354, 1396, 1479 (s)[g]	806 (o)		1593	1911	3031, 3061		
35a		1139	1006 (i), 1475 (s)			1163		3036, 3063		
36a		1072, 1128	1003 (i), 1408, 1477			1664		3035, 3061		
5a		1010 (o), 1132, 1279	1481 (s),[g] 1579	819 (o)	1250			3032, 3061		
6a		982, 1101, 1134, 1230, 1281	1381, 1466 (s)[g]	810 (o)	752, 1686	1560	1884	3102		
11a	777	1122, 1273	1024 (i), 1362, 1406, 1454	806 (o)		1603, 1670		3045		
14a[e]			1432	795 (o), 1045	997			3080		
16a[e]			1432	799 (o), 899 (o), 1046	735, 786, 979			3080		
38a[e]			1197, 1432, 1493	797 (o), 845 (o), 1051	736, 986, 1007			3076		
18a		879	1034 (i), 1385, 1470		748, 1659	1512, 1610		3035, 3059		
31a	733	876, 1045	1012 (i), 1402, 1481	798 (o)	798, 1659	1591, 1608	1874	3074		
23a		957, 1261	1431, 1489	812, 850 (o)	704, 995, 1672	1605		3076, 3097		
20a		879	1360, 1466, 1504, 1672					(C−F) 748 (i), (C−F str) 1036		
32a		1215	1010 (i), 1402, 1483	793	793, 958	1587		3066		
12a	787		1356, 1468			1603, 1672	1743			
26a[f]	707	1078	1012 (i), 1360, 1396, 1491 (i), 2210 (C≡C)	825		1587		3056		

[a] The structure is given in the text; compounds are arranged by similarity. [b] a = asymmetric mode, s = symmetric mode, sc = scissoring mode, o = out-of-plane mode, i = in-plane mode. [c] Reference 34. [d] Reference 77. [e] Reference 74. [f] References 26 and 33. [g] Reference 82.

4,4′-Dimercaptooctafluorobiphenyl (**20a**) displays C=C ring stretch modes that are similar, although shifted and less intense, to those of its hydrogenated analogue (4,4′-dimercaptobiphenyl (**8a**)) and features in addition quite strong C−F stretch modes. Ellipsometry measurements demonstrate that its layer thickness is much lower than

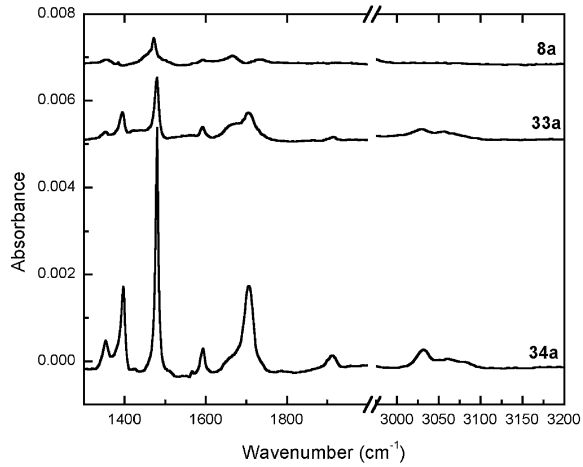

Figure 3. GI-FTIR spectra of aromatic C═C and C−H stretch modes of biphenyldithiol (**8a**), terphenyldithiol (**33a**), and quaterphenyldithiol (**34a**). A vertical offset is introduced for clarity (0.005 and 0.007 units for **33a** and **8a**, respectively).

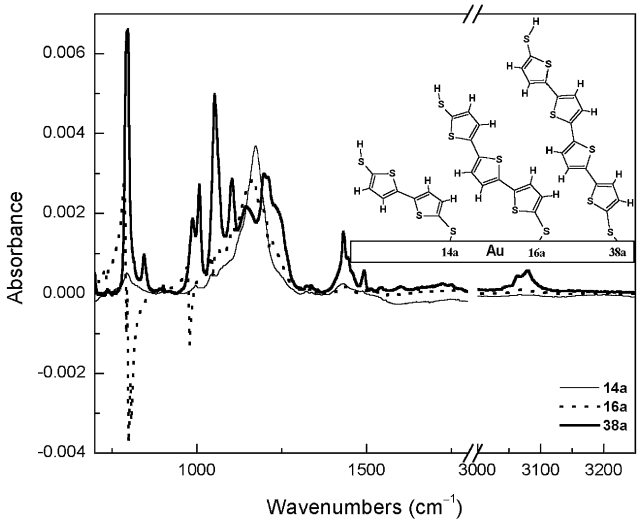

Figure 4. GI-FTIR spectra of the C−S, C−C−H, and C−H stretch modes of bithiophenedithiol (**14a**), terthiophenedithiol (**16a**), and quaterthiophenedithiol (**38a**). The inset shows schematically the orientation of **14a**, **16a**, and **38a** on the gold surface.

the end-to-end length of the molecule. On the basis of these measurements, we conclude that **20a** is more tilted than **8a**.

A very strong stretch mode around 1250 cm^{-1} is observed for compound **5a** in the GI-FTIR spectrum and is assigned to the C−O ether stretching. The ether stretch mode should only be detectable if the C−O−C bonds are not parallel to the surface, so its strong intensity suggests that **5a** is oriented close to the surface normal. Ellipsometric data confirm that the layer thickness is only slightly less than the length of the molecule (Table 3).

Compounds **12a**, **22a**, **26a**, and 1,4-benzenedithiol give low-intensity absorption bands in GI-FTIR, but certain specific modes can still be assigned (Table 2). We conclude, based on GI-FTIR, ellipsometry, and contact angle measurements (all compounds demonstrate a hydrophilic effect at the surface), that all four compounds (**12a**, **22a**, **26a**, and 1,4-benzenedithiol) are not lying flat on the surface but have a definite tilt angle with one thiol group bound to gold and the other pointing upward.

In Figure 4, the GI-FTIR spectra of the oligo(thiophene)-dithiol series are presented, demonstrating a more complex behavior for this series than for the phenylene-based dithiols. First, the GI-FTIR spectrum of a SAM of terthiophenedithiol shows "antiabsorption" or negative bands that are assigned to C−S stretch modes (735, 786, and 979 cm^{-1}) and C−H out-of-plane (799, 899, and 1046 cm^{-1}) modes. For *monolayers* on metal substrates, such unusual (Fano) bands have so far only been observed in a few cases of atomic and diatomic adsorbates.[84,85] They are due to nonadiabatic interactions between an adsorbate vibrational mode and the surface electronic states or conduction electrons in the metal substrate, giving rise to narrow, highly asymmetric or negative features in the surface infrared absorption spectrum.[84,85] In the present case, C−S antiabsorption bands might therefore indicate a specific chemical interaction of one or more thiophene rings of terthiophenedithiol with the Au substrate, most likely through a Au−S bond. If this infrared absorption mechanism applies, the antiabsorption bands should be accompanied by an increase in the broadband infrared absorption spanning the entire wavenumber regime probed. Such small broadband reflectivity changes, however, are not easy to quantify experimentally due to baseline fluctuations. To clarify the exact nature of these observed antiabsorption bands, more research will be conducted.

Second, the C═O mode at 1750 cm^{-1} has disappeared, confirming the complete deprotection of the thioacetyl end group. Third, a broad band appeared around 1165 cm^{-1}, which is assigned to an oxidized species (probably a sulfone) as mentioned above. Finally, similarly to the oligo(phenylene) series, the intensity of the C−C and C−H modes increased more than linearly with increasing chain length, implying that the longer terthiophenedithiol and quaterthiophenedithiol have a smaller tilt angle α than bithiophenedithiol. The increased intensity of the C−H out-of-plane mode (~800 cm^{-1}) is attributed to a difference of the rotation angle β. As mentioned above, a small but nonzero tilt angle α can yield quite strong out-of-plane C−H modes, especially if the rotation angle β is close to 0° (Figure 2D). Therefore, it is proposed that the tilt angle decreases with increasing number of thiophene units and that the rotation angle is close to zero for the thiophene-based dithiols. Ellipsometry measurements confirm this proposal, as the measured layer thickness of **14a** is much smaller than the calculated length of the molecule, whereas the measured layer thickness of **38a** is almost equal to the molecular length, and terthiophene **16a** represents the intermediate scenario.

Contact Angle Measurement. Contact angle measurement is a simple and useful technique to determine the macroscopic surface properties of thin films.[9,10,51,81] An increase in the contact angle of water for different lengths of oligophenylene adsorbates was used to prove an "edge-on" orientation of densely packed SAMs. Table 3 summarizes the advancing, receding, and static contact angles of water and hexadecane (HD) on the SAM-modified surfaces. Compared with the alkanethiols, aromatic thiols are more hydrophilic as indicated by the lower contact angles in Table 3. The conjugated thiols are almost fully wetted by hexadecane.[81] Increasing the chain length of conjugated thiols reduces the dipole moment formed on the surface, which, in turn, results in a more hydrophobic character of the longer ring system. This is demonstrated by the increase of the advancing, receding, and static angles with the length of the self-assembled molecule

(84) (a) Chabal, Y. J. *Phys. Rev. Lett.* **1985**, *55*, 845. (b) Reutt, J. E.; Chabal, Y. J.; Christman, S. B. *Phys. Rev. B* **1988**, *38*, 3112.
(85) (a) Persson, B. N. J.; Volokitin, A. I. *Surf. Sci.* **1995**, *310*, 314. (b) Volotkin, A. I.; Persson, B. N. *J. Phys. Rev. B* **1995**, *52*, 2899.

Table 3. Preparation Conditions, Calculated Molecular Length, and Ellipsometry and Contact Angle Goniometry Data on Conjugated Mono- and Dithiols

compound[a]	concn[b] ($\times 10^{-5}$ M)	dissolves or precipitates[c]	calculated molecular length[d] (Å)	measured layer thickness (Å)[e]	contact angle H_2O[f] (deg)			contact angle hexadecane[f] (deg)		
					Θ_A	Θ_R	Θ_S	Θ_A	Θ_R	Θ_S
cleaned gold					93	38	58	8	3	6
$C_{16}H_{33}SH$	50	S	24.7	17.2[g]	102	90	97	35	13	26
22a	5	S	9.4	9.9 ± 0.7	75	36	66	7	4	5
$HS-C_6H_4-SH$	5	S	9.0	3.8 ± 0.5	73	36	60	7	3	5
8a	5	P	13.3	9.7 ± 1.1	81	40	68	6	3	4
33a	5	P	17.6	13.7 ± 1.9	79	40	68	7	3	5
34a	1	P	21.8	22.1 ± 1.3	87	48	74	5	3	4
35a	5	S	12.3	7.2 ± 1.3	92	66	80	8	3	4
36a	5	S	16.6	17.9 ± 1.3	94	59	73	9	4	6
5a	5	S	13.3	11.2 ± 0.8	76	28	67	6	4	5
6a	5	S	13.5	12.5 ± 1.3	76	29	63	5	3	4
11a	5	S	13.3	11.1 ± 2.2	84	46	70	9	4	5
14a	5	S	12.6	7.3 ± 0.6	64	25	55	8	4	5
16a	5	S	16.6	10.9 ± 1.0	78	39	73	5	2	4
38a	1	P	20.1	18.7 ± 1.2	95	59	75	6	3	4
18a	5	S	16.9	11.9 ± 2.9	77	39	69	5	3	4
31a	5	S	17.1	19.3 ± 0.9	84	36	72	6	3	4
23a	5	P	15.7	21.0 ± 0.8	97	45	74	8	3	5
20a	5	S	13.5	5.3 ± 0.8	78	38	69	7	3	5
32a	1	P	20.4	27.1 ± 1.3	78	53	67	7	4	5
12a	5	S	9.7	9.3 ± 1.0	79	48	70	7	3	5
26a	5	S	15.8	19.5 ± 0.4	96	58	71	4	3	3

[a] The structure is given in the text; compounds are arranged by similarity. [b] In THF. [c] Indicates whether the deprotected compound is soluble (S) or whether it precipitates (P) after several weeks at given concentration in THF. [d] Defined as the distance from Au to the farthest hydrogen atom of the molecule, optimized by the PM3 semiempirical method (see Experimental Section). [e] Measured by ellipsometry assuming a refractive index of 1.55. [f] Θ_A = advancing contact angle, Θ_R = receding contact angle, Θ_S = static contact angle. [g] Refractive index of 1.45.

(compare ter- (**16a**) and quaterthiophenes (**38a**) or ter- (**33a**) and quaterphenyl (**34a**)).

The large difference in the contact angle of water for dithiols **18a**, **8a**, and **33a** compared to their analogous monothiols **23a**, **35a**, and **36a**, respectively, must be related to hydrophilic SH groups present on the surface of the dithiol SAM, which is consistent with an edge-on monolayer structure with only one terminal thiol group being attached to a gold surface.[10,23,37] Similar trends have been observed in aromatic diisocyanide SAMs.[86]

Although the packing density will influence the orientation at a small length scale, GI-FTIR spectrometry, ellipsometry, contact angle measurement, and electrochemistry probe surface areas of at least several mm^2, and therefore the observations made and the conclusions drawn are valid for the overall orientation in SAMs of conjugated mono- and dithiols.

Conclusions

A series of aromatic and heteroaromatic acetyl-protected mono- and dithiol compounds with varied lengths and different aromatic backbones have been synthesized and characterized. UV−vis spectroscopy showed a red-shifted absorption maximum with increasing chain length, especially when thiophene rings were introduced in the conjugated molecule. Obviously, the optical band gap was also lowered when the aromatic system was extended. The redox behavior of the conjugated SAMs was investigated, and data on terthiophenedithiol were discussed in more detail. The electrochemical behavior in solution of the aromatic thioacetyl derivatives studied was represented by a multielectron irreversible or partially quasi-reversible oxidation wave, and the potentials are strongly dependent on the π-conjugated length of the molecule. The electrochemistry of terthiophenedithiol in a SAM and in solution exhibits a partially reversible oxidation wave. The formation of self-assembled monolayers of these conjugated mono- and dithiol compounds on gold was achieved by in situ deprotection of the corresponding acetylated derivatives. The resulting SAMs were studied by grazing incidence FTIR, contact angle, and ellipsometry measurements, confirming the formation of edge-on monolayer structures. On the basis of the combined data from GI-FTIR, ellipsometry, and contact angle measurements, we conclude that increasing the chain length of conjugated dithiol molecules results in a less tilted molecular orientation with respect to the surface normal. GI-FTIR showed a more than linear increase of the aromatic C−C stretch modes when the chain length was increased from two to four phenyl rings, indicating that the longer *p*-phenylene system is oriented along the surface normal. Similarly, increasing the length of the thiophene oligomers from two to four rings resulted in a more than linear increase of the intensity of the C−C stretch and C−H bend modes, again implying that the longest oligothiophenedithiol molecules are aligned very close to the surface normal, which is also corroborated by ellipsometry measurements.

Experimental Section

General Methods. All chemical reagents were purchased from Aldrich Chemical Co. unless otherwise stated. 1,4-Benzenedithiol was purchased from Tokyo Kasei Kogyo Co., Ltd. Elemental analysis was performed by Robertson Microlit Laboratories (Madison, NJ). Nuclear magnetic resonance (NMR) spectra were taken on a Bruker 360 MHz spectrometer. All chemical shifts were reported relative to tetramethylsilane (TMS) at 0.0 ppm. UV−vis spectra were obtained on a HP-8453 spectrometer. Mass spectra were taken on a VG/Micromass Autospec with a 70 eV source (200 °C).

Self-Assembled Monolayer Formation. Gold-coated (1000 Å thickness) silicon wafers with a 100 Å titanium adhesion layer were prepared by e-beam deposition. Prior to submersion into the thiol-containing THF (anhydrous) solution, the gold sub-

(86) Henderson, J. I.; Feng, S.; Bein, T.; Kubiak, C. P. *Langmuir* **2000**, *16*, 6183.

strates were cleaned for 30 min in a mixture of water/NH_4OH/H_2O_2 (5:1:1) held at 75 °C, rinsed with deionized water (3 times), and blown dry with N_2. In a glovebox under argon, the acetyl-protected molecules were dissolved in THF ($\sim 5 \times 10^{-5}$ M, see Table 3), deprotected by adding 1 drop of 30% ammonium hydroxide (aq) per 10 mL of THF solution, and filtered through a 0.2 μm Teflon membrane. The gold substrates were immersed into the solution with the gold layer facing down. After immersion for at least 2 days, the substrates were thoroughly rinsed with THF, toluene, and 2-propanol, dried with a N_2 flow, and measured immediately.

Grazing Incidence FT-IR. The GI-FTIR data were recorded under a nitrogen atmosphere in a Nicolet 760 spectrometer equipped with a grazing incidence module containing gold-coated silicon wafers as mirrors at an 85° angle. Before measurement of the SAMs on gold-coated silicon wafers, a reference spectrum was recorded on a freshly cleaned (the cleaning procedure is described above) gold substrate. Two thousand consecutive scans were averaged before the spectrum was corrected for the gold substrate by plotting the absorbance as $-\log(R/R_0)$, where R is the reflectivity of the substrate with the monolayer and R_0 is the reflectivity of the reference gold substrate. The nominal spectral resolution was set at 4 cm^{-1}.

Ellipsometry. Layer thicknesses were measured on a Rudolph research/auto EL ellipsometer equipped with a He−Ne laser (λ = 632.8 nm) at an incidence angle of 70° with respect to the surface normal. Optical constants of the gold-coated substrates were measured prior to the SAM measurements and calculated from the ellipsometric parameters delta ($\Delta = \delta_1 - \delta_2$), defined as the phase difference between the p-wave and the s-wave before (δ_1) and after the reflection (δ_2), and psi ($\tan \psi = |R^p|/|R^s|$), where ψ is the angle whose tangent is the ratio of the magnitudes of the total reflection coefficients with R^p being the reflection coefficient of the p-wave and R^s the reflection coefficient for the s-wave.[87] The SAMs were rinsed with deionized water and 2-propanol three times and dried for 5 min with N_2 before collecting the data. All layer thicknesses reported were calculated after averaging over at least five measurements. The refractive index of the conjugated monolayer was assumed to be isotropic and estimated to be 1.55,[73] and for hexadecanethiol a refractive index of 1.45 was used.[35]

Contact Angle Measurements. The advancing, receding, and static contact angles of deionized water (>18 MΩ cm) and HD were measured on a Ramé-Hart, Inc., NRL contact angle goniometer (model 100-00) and averaged over at least five spots. The advancing angles are produced as fluid is added to the drop, and the receding angles as fluid is withdrawn.

Cyclic Voltammetry (CV) Measurements. CV experiments were performed on a BAS 100B electrochemical analyzer in an argon-filled glovebox with a three-electrode cell in a CH_2Cl_2 solution (0.2 M Bu_4NPF_6 as an electrolyte) at different scan rates (10−1000 V s^{-1}). A platinum wire and a Ag/Ag^+ electrode were used as the counter and reference electrodes, respectively. The oxidation of ferrocene under our conditions occurs at $E_{ox}{}^0 = +0.24$ V versus Ag/Ag^+ (0.50 V vs Ag/AgCl and 0.44 V vs SCE). A glassy carbon electrode (BAS, d = 2.5 mm) was used as a working electrode for studying the solution electrochemistry, and gold disk electrodes (BAS, d = 1.6 mm, and homemade, d = 6.0 mm) with self-assembled monolayers were used to record the CV of SAMs. The thiol monolayer was self-assembled on gold electrodes as described above.

Semiempirical calculations were performed on the PM3 level using HyperChem 6.03 software. The self-assembled thiols were fully optimized to the RMS gradient 0.005 kcal $Å^{-1}$ mol^{-1}. The optimization was run from several initial conformations to make sure the global minimum was found. The maximal monolayer thickness was estimated as the distance from the Au atom to the farthest hydrogen atom in the optimized molecule. S−Au and Se−Au bonds were constrained to 2.36 and 2.50 Å, respectively; the C−S(Se)−Au angle was constrained to 180°.

Disulfonyl Chloride 3. Chlorosulfonic acid (20 mL) was slowly added to diphenyl ether **1** (8.5 g, 0.050 mol), and the reaction mixture was stirred for 2 h at room temperature. The mixture was then poured into ice water (200 mL), and the crude disulfonyl chloride was collected by filtration. The white solid was thoroughly washed with water and dried in vacuo to give the crude compound **3** (15.6 g, 85%),[54] which was used in the next step without further purification. m/z (EI): 366 (M^+, 100%). ^1H NMR ($CDCl_3$): δ 8.13 (d, J = 7.3 Hz, 4 H), 7.30 (d, J = 7.3 Hz, 4 H) ppm. ^{13}C NMR ($CDCl_3$): δ 160.7, 140.0, 130.0, 119.8 ppm.

Disulfonyl Chloride 4. This compound was prepared using similar procedures as for compound **3** from diphenylsulfide (**2**) (yield, 80%). m/z (EI): 382 (M^+, 100%). ^1H NMR ($CDCl_3$): δ 8.01 (d, J = 7.7 Hz, 4 H), 7.57 (d, J = 7.7 Hz, 4 H) ppm. ^{13}C NMR ($CDCl_3$): δ 143.8, 143.6, 131.3, 128.1 ppm.

Dithiol 5a. Disulfonyl chloride **3** (8.5 g, 0.023 mol) was added to a solution of sulfuric acid (98%; 100 g) in water (200 mL) with vigorous stirring at room temperature, followed by a freshly prepared zinc dust amalgam (50 g, excess).[55] After being stirred for 2 h, the mixture was refluxed for an additional 3 h. The reaction mixture was then cooled to room temperature and extracted with benzene. The solvent was evaporated to yield a white solid, which was purified by sublimation to give dithiol **5a** (4.1 g, 78%), mp 100−102 °C. m/z (EI): 234 (M^+, 100%). ^1H NMR ($CDCl_3$): δ 7.29 (d, J = 7.3 Hz, 4 H), 6.90 (d, J = 7.3 Hz, 4 H), 3.43 (s, 2 H) ppm. ^{13}C NMR ($CDCl_3$): δ 155.7, 131.8, 124.1, 119.6 ppm. Anal. Calcd for $C_{12}H_{10}OS_2$ (234.3 g/mol): C, 61.50; H, 4.30; S, 27.37. Found: C, 61.27; H, 4.30; S, 26.97.

Dithiol 6a. This compound was prepared using similar procedures as for compound **5a** from sulfonyl chloride **4** (yield, 89%), mp 104−105 °C. m/z (EI): 250 (M^+, 100%). ^1H NMR ($CDCl_3$): δ 7.18 (b, 8 H), 3.46 (s, 2 H) ppm. ^{13}C NMR ($CDCl_3$): δ 133.0, 131.7, 130.1, 127.1 ppm. Anal. Calcd for $C_{12}H_{10}S_3$ (250.4 g/mol): C, 57.56; H, 4.03; S, 38.42. Found: C, 56.30; H, 3.89; S, 36.03.

Dithioacetyl 5. Compound **5a** (1.5 g, 6.6 mmol) and acetyl chloride (1.3 g, 16 mmol) were dissolved in anhydrous diethyl ether (50 mL). To this solution was added triethylamine (1.7 g, 16 mmol). The reaction mixture was refluxed for 3 h, and the resulting white precipitate was filtered and washed with diethyl ether (2 × 20 mL). The filtrate was washed with water and then dried with $MgSO_4$, and the solvent was evaporated to give the crude product **5** which was further purified by flash chromatography on silica gel with hexane/methylene chloride (1:1 v/v) to give white crystals of **5** (1.9 g, 90%), mp 67−68 °C. m/z (EI): 318 (M^+, 100%). ^1H NMR ($CDCl_3$): δ 7.39 (d, J = 7.3 Hz, 4 H), 7.09 (d, J = 7.3 Hz, 4 H), 2.43 (s, 6 H) ppm. ^{13}C NMR ($CDCl_3$): δ 194.3, 157.7, 136.2, 122.4, 119.7, 30.1 ppm. Anal. Calcd for $C_{16}H_{24}O_3S_2$ (318.3 g/mol): C, 60.35; H, 4.43; S, 20.14. Found: C, 60.40; H, 4.37; S, 20.17.

Dithioacetyl 6. This compound was prepared using similar procedures as for compound **5** from **6a** (yield, 68%): white crystals, mp 68−69 °C. m/z (EI): 334 (M^+, 100%). ^1H NMR ($CDCl_3$): δ 7.35 (b, s, 8 H), 2.43 (s, 6 H) ppm. ^{13}C NMR ($CDCl_3$): δ 193.6, 137.0, 135.1, 131.4, 127.0, 30.2 ppm. Anal. Calcd for $C_{16}H_{14}O_2S_3$ (334.5 g/mol): C, 57.45; H, 4.22; S, 28.76. Found: C, 57.54; H, 4.09; S, 28.55.

Dithiol 8a. This compound was prepared using similar procedures as for compound **5a** from 4,4′-biphenyldisulfonyl chloride **7** (yield, 83%), mp 174 °C. m/z (EI): 218 (M^+, 100%). ^1H NMR ($CDCl_3$): δ 7.42 (d, J = 8.4 Hz, 4 H), 7.32 (d, J = 8.4 Hz, 4 H), 3.47 (s, 2 H) ppm. ^{13}C NMR ($CDCl_3$): δ 138.0, 130.0, 129.9, 127.4 ppm (the resonance at 129.9 was only observed with long acquisition time due to the long relaxation time of this quaternary carbon). Anal. Calcd for $C_{12}H_{10}S_2$ (218.3 g/mol): C, 66.01; H, 4.62; S, 29.37. Found: C, 65.88; H, 4.54; S, 29.07.

Dithioacetyl 8. This compound was prepared from **8a** using similar procedures as for compound **5** (yield, 94%), mp 113 °C. m/z (EI): 302 (M^+, 100%). ^1H NMR ($CDCl_3$): δ 7.60 (d, J = 8.2 Hz, 4 H), 7.48 (d, J = 8.2 Hz, 4 H), 2.43 (s, 6 H) ppm. ^{13}C NMR ($CDCl_3$): δ 193.6, 141.3, 134.7, 127.9, 127.6, 30.1 ppm. Anal. Calcd for $C_{16}H_{14}O_2S_2$ (302.3 g/mol): C, 63.55; H, 4.67; S, 21.21. Found: C, 63.63; H, 4.53; S, 20.63.

Disulfonyl Chloride 10. To a stirred solution of fluorene **9** (8.3 g, 0.050 mol) in acetic acid (50 mL), chlorosulfonic acid (15.5 g, 0.15 mol) was added dropwise at 0 °C. The reaction mixture was refluxed for 2 h, cooled, and poured into a saturated aqueous solution of NaCl (200 mL) containing NaOH (5.0 g, 0.13 mol).

(87) *Spectroscopic Ellipsometry and Reflectometry*: *A User's Guide*; Tompkins, H. G., McGahan, W. A., Eds.; John Wiley & Sons: New York, 1999.

The precipitate was washed with a saturated solution of NaCl (3 × 30 mL) and dried overnight at 60 °C in vacuo to give sodium fluorene-2,7-disulfonate (13.0 g, 70%). ^{1}H NMR (D_2O): δ 7.68 (s, 2 H), 7.59 (d, J = 8.0 Hz, 2 H), 7.46 (d, J = 8.0 Hz, 2 H), 3.36 (s, 2 H) ppm. ^{13}C NMR (D_2O): δ 145.0, 142.9, 142.0, 124.7, 122.4, 121.0, 36.8 ppm. The salt (3.7 g, 0.010 mol) was mixed with phosphorus pentachloride (5.2 g, 0.25 mol) and stirred at 120 °C for 2 h.[88] The phosphorus oxychloride formed during the reaction was distilled off, and the resulting dry residue was pulverized in a mortar and then treated with water. The precipitate was filtered off and washed with water to give disulfonyl chloride **10** (2.5 g, 69%) as a light-reddish-brown powder. m/z (EI): 362 (M^+, 60%). ^{1}H NMR ($CDCl_3$): δ 8.30 (s, 1 H), 8.19 (d, J = 8.3 Hz, 2 H), 8.11 (d, J = 8.3 Hz, 2 H), 4.20 (s, 2 H) ppm. ^{13}C NMR ($CDCl_3$): δ 143.0, 142.8, 141.0, 124.2, 121.6, 119.6, 34.7 ppm.

Dithiol 11a. Stannous chloride dihydrate (25 g, 0.22 mol) was dissolved in a mixture of acetic anhydride (100 mL) and concentrated HCl (20 mL), the mixture was heated to 80−90 °C, and disulfonyl chloride **10** (1.81 g, 5.0 mmol) was added with stirring. The reaction temperature was kept at 90 °C for 2 h. The reaction mixture was then allowed to cool to 20 °C and then poured into water (100 mL) containing concentrated HCl (20 mL). The light-yellow precipitate was filtered, washed with water, and dried to yield dithiol **11a** (1.05 g, 92%). m/z (EI): 230 (M^+, 100%). ^{1}H NMR ($CDCl_3$): δ 7.57 (d, J = 7.9 Hz, 2 H), 7.44 (s, 2 H), 7.29 (d, J = 7.9 Hz, 2 H), 3.81 (s, 2 H), 3.50 (s, 2 H) ppm. ^{13}C NMR ($CDCl_3$): δ 143.8, 139.2, 128.4, 128.3, 126.5, 120.1, 36.43 ppm.

Dithioacetyl 11 was prepared from crude dithiol **11a** using similar procedures as described for compound **5**: white powder (yield, 90%), mp 142−143 °C. m/z (EI): 314 (M^+, 100%). ^{1}H NMR ($CDCl_3$): δ 7.80 (d, J = 7.9 Hz, 2 H), 7.59 (s, 2 H), 7.43 (d, J = 7.9 Hz, 2 H), 3.93 (s, 2 H), 2.42 (s, 6 H) ppm. ^{13}C NMR ($CDCl_3$): δ 194.0, 144.3, 142.1, 133.2, 131.1, 126.8, 120.7, 36.7, 30.0 ppm. Anal. Calcd for $C_{17}H_{14}O_2S_2$ (314.4 g/mol): C, 64.94; H, 4.49; S, 20.40. Found: C, 64.91; H, 4.33; S, 20.18.

Dithioacetyl 12. 1,5-Naphthalenedithiol **12a** was prepared according to refs 88 and 55. 1,5-Naphthalenedithiol **12a** was protected using a similar procedure as described for compound **5**: white crystals (yield, 63%), mp 185−186 °C. m/z (EI): 276 (M^+, 100%). ^{1}H NMR ($CDCl_3$): δ 8.35 (d, J = 8.7 Hz, 2 H), 7.75 (d, J = 7.0 Hz, 2 H), 7.58 (m, 2 H), 2.46 (s, 6 H) ppm. ^{13}C NMR ($CDCl_3$): δ 193.1, 135.5, 135.0, 128.2, 126.6, 126.5, 30.1 ppm. Anal. Calcd for $C_{14}H_{12}O_2S_2$ (276.30 g/mol): C, 60.84; H, 4.38; S, 23.20. Found: C, 60.60; H, 4.29; S, 22.92.

Dithioacetyl 14. Into a solution of (5,5′)-bis(magnesium bromide)-(2,2′)-bithiophene (0.02 mol), prepared by the reaction of (5,5′)-dibromo-(2,2′)-bithiophene (**13**) (6.48 g, 0.02 mol) with Mg (1.06 g, 0.044 mol) in 60 mL of dry ether, was added sulfur powder (1.40 g, 0.044 mol) in one portion at −78 °C. The reaction mixture was warmed to 0 °C for 30 min and then recooled to −78 °C, and acetyl chloride (7.02 g, 0.080 mol) was added in one portion. The reaction mixture was allowed to warm to 20 °C, stirred at this temperature overnight, and then poured into water (100 mL) and extracted with diethyl ether (3 × 50 mL). The combined organic solution was washed with water and saturated NaCl and dried over $MgSO_4$. After removal of the solvent, the residue was purified by flash chromatography on silica with hexane/methylene chloride (1:1 v/v) as the eluant followed by recrystallization from hexane/ethyl acetate to give a light-yellow solid **14** (1.63 g, 26%), mp 133−135 °C. ^{1}H NMR ($CDCl_3$): δ 7.16 (d, J = 3.8 Hz, 2 H), 7.06 (d, J = 3.8 Hz, 2 H), 2.42 (s, 6 H) ppm. ^{13}C NMR ($CDCl_3$): δ 193.7, 142.4, 136.3, 124.8, 124.7, 29.5 ppm.

Dithioacetyl 16. Terthiophene **15** (1 g, 4 mmol) was refluxed with a solution of *n*-BuLi (2.5 M solution in hexane; 4 mL, 10 mmol) for 2 h and cooled to −78 °C, and sulfur powder (0.32 g, 10 mmol) was added in one portion. The reaction mixture was warmed to 0 °C for 30 min and then recooled to −78 °C, and acetyl chloride (1.17 g, 15 mmol) was added in one portion. The reaction mixture was allowed to warm to 20 °C and stirred at this temperature overnight. The solvent was removed in vacuo, and the residue was purified by flash chromatography on silica with hexane/methylene chloride (1:1 v/v) as the eluant followed by recrystallization from hexane to give a light-yellow solid **16** (0.50 g, 31%), mp 143−144 °C. m/z (EI): 396 (M^+, 100%). ^{1}H NMR ($CDCl_3$): δ 7.25 (s, 4 H), 7.13 (d, J = 3.8 Hz, 2 H), 7.05 (d, J = 3.8 Hz, 2 H), 2.41 (s, 6 H) ppm. ^{13}C NMR ($CDCl_3$): δ 193.4, 142.8, 136.3, 136.2, 125.1, 124.5, 124.2, 29.3 ppm. Anal. Calcd for $C_{16}H_{12}O_2S_5$ (396.5 g/mol): C, 48.46; H, 3.05; S, 40.43. Found: C, 48.24; H, 2.74; S, 40.59.

1,4-Bis(2-thienyl)benzene 17 was prepared from 2-bromothiophene and 1,4-benzenediboronic acid according to standard procedures for Suzuki reactions:[89] orange-yellow solid (yield, 90%), mp 197−200 °C. ^{1}H NMR ($CDCl_3$): δ 7.61 (s, 4 H), 7.32 (dd, J = 3.6 Hz, 1.1 Hz, 2 H), 7.27 (dd, J = 3.6 Hz, 1.1 Hz, 2 H), 7.07 (m, 2H) ppm. ^{13}C NMR ($CDCl_3$): δ 143.9, 133.5, 128.0, 126.3, 124.8, 123.1 ppm. Anal. Calcd for $C_{14}H_{10}S_2$ (242.4 g/mol): C, 69.38; H, 4.16; S, 26.46. Found: C, 69.22; H, 3.86; S, 26.36.

Dithioacetyl 18 was synthesized from compound **17** using similar procedures as described for compound **16**: yellow powder (yield, 42%), mp 186−188 °C. m/z (EI): 390 (M^+, 100%). ^{1}H NMR ($CDCl_3$): δ 7.59 (s, 4 H), 7.30 (d, J = 3.8 Hz, 2 H), 7.13 (d, J = 3.8 Hz, 2 H), 2.42 (s, 6 H) ppm. ^{13}C NMR ($CDCl_3$): δ 193.6, 149.8, 136.6, 133.5, 126.4, 124.8, 123.8, 29.3 ppm. Anal. Calcd for $C_{18}H_{12}O_2S_4$ (390.5 g/mol): C, 55.35; H, 3.61; S, 32.84. Found: C, 55.43; H, 3.48; S, 32.51.

Dithioacetyl 20. To a solution of *n*-BuLi (2.5 M solution in THF, 5.0 mL, 0.013 mol) in dry THF (50 mL) at −78 °C was added dropwise a solution of **19** (2.3 g, 5.0 mmol) in dry THF (20 mL). The mixture was warmed to 20 °C, stirred for 2 h, and then cooled to −78 °C. Sulfur powder (0.48 g, 0.015 mol) was then added in one portion. The reaction mixture was warmed to 0 °C, stirred for 30 min, and then cooled to −78 °C. Acetyl chloride (1.2 g, 0.015 mol) was added in one portion. After warming up to 20 °C and stirring overnight, the solvent was removed in vacuo and the residue was purified by flash chromatography on silica gel with hexane/methylene chloride (1:1 v/v) as the eluant followed by recrystallization from hexane to afford a light-yellow solid **20** (1.50 g, 67%), mp 137−139 °C. m/z (EI): 446 (M^+, 100%). ^{1}H NMR ($CDCl_3$): δ 2.54 (s, 6 H) ppm. ^{13}C NMR ($CDCl_3$): δ 187.8, 147.9, 145.5, 145.2, 142.7, 142.5, 110.8, 110.6, 110.3, 109.2, 30.2 ppm. Anal. Calcd for $C_{16}H_6F_8O_2S_2$ (446.3 g/mol): C, 43.06; H, 1.35; S, 14.37; F, 34.05. Found: C, 43.01; H, 1.41; S, 14.43; F, 33.85.

1,4-(Diacetylseleno)benzene 22. To a solution of 1,4-dibromobenzene **21** (6.13 g, 26.0 mmol) in 100 mL of dry THF at −78 °C was added *t*-BuLi (1.7 M solution in pentane, 61.2 mL, 104 mmol). The reaction mixture was stirred for 2 h and warmed to 0 °C for 30 min, and Se powder (4.10 g dispersed in 30 mL of dry THF, 52 mmol) was added in 30 min. Then the solution was recooled to −78 °C, acetyl chloride (4.3 mL, 60 mmol) was added, and the solution was warmed to room temperature and stirred for 14 h. THF, pentane, and acetyl chloride were evaporated, and the residue was dissolved in 50 mL of dichloromethane and washed with 2 × 50 mL of water. The organic phase was dried over $MgSO_4$, and solvent evaporation yielded an orange solid, which was purified by flash chromatography on silica with hexane/methylene chloride (1:1 v/v) as the eluant followed by recrystallization from hexane to give the orange product **22** (2.70 g, 32%), mp 116−118 °C. ^{1}H NMR ($CDCl_3$): δ 7.49 (s, 4 H), 2.46 (s, 6 H). ^{13}C NMR ($CDCl_3$): δ 195.5, 136.2, 127.9, 34.2 ppm. m/z (EI): 322 (M^+, 100%), 320 (M^+, 90%), 318 (M^+, 60%) (Isotope pattern of Se). Anal. Calcd for $C_{10}H_{10}O_2Se_2$ (320.10 g/mol): C, 37.52; H, 3.15; Se, 49.33. Found: C, 37.28; H, 2.93; Se, 50.22.

Monothioacetyl 23. 1,4-Bis(2-thienyl)benzene **17** (1.091 g, 4.5 mol) was refluxed with a solution of *n*-BuLi (2.5 M solution in ether; 1.8 mL, 4.5 mmol) for 2 h and cooled to −78 °C, and sulfur powder (0.16 g, 5.0 mmol) was added in one portion. The reaction mixture was warmed to 0 °C for 30 min and then cooled to −78 °C, and acetyl chloride (0.52 g, 7.5 mmol) was added in one portion. The reaction mixture was allowed to warm to 20 °C and stirred at this temperature overnight. The solvent was removed in vacuo, and the residue was purified by flash chromatography on silica with hexane/methylene chloride (1:1 v/v) as the eluant followed by recrystallization from hexane/ethyl acetate to give a light-yellow solid **23** (0.854 g, 60%), mp 178−180 °C. m/z (EI): 316 (M^+, 100%). ^{1}H NMR ($CDCl_3$): δ 7.63

(88) Ceasar, P. D. *Org. Synth. Coll. IV* **1963**, 693.

(89) Miyaura, N.; Suzuki, A. *Chem. Rev.* **1995**, *95*, 2457.

(d, J = 8.6 Hz, 2 H), 7.59 (d, J = 8.6 Hz, 2 H), 7.34 (d, J = 3.6 Hz, 1 H), 7.30 (m, 2 H), 7.13 (d, J = 3.8 Hz, 1 H), 7.09 (m, 1 H), 2.42 (s, 3 H) ppm. ^{13}C NMR ($CDCl_3$): δ 193.7, 149.5, 144.25, 143.9, 143.7, 136.6, 128.0, 126.3, 125.0, 123.6, 123.3, 29.3 ppm.

Dithioacetyl 26 was prepared using the same procedures as described in the literature:[61] white powder (yield, 37%), mp 125−126 °C. m/z (EI): 326 (M^+, 100%). ^{1}H NMR ($CDCl_3$): δ 7.54 (d, J = 8.3 Hz, 4 H), 7.39 (d, J = 8.3 Hz, 4 H), 2.41 (s, 6 H) ppm. ^{13}C NMR ($CDCl_3$): δ 193.3, 134.2, 132.2, 128.4, 124.1, 90.2, 30.3 ppm. Anal. Calcd for $C_{18}H_{14}O_2S_2$ (326.4 g/mol): C, 66.23; H, 4.32; S, 18.82. Found: C, 66.11; H, 4.25; S, 18.34.

Dithiol 31a. To a mixture of 4-(methylthio)phenylboronic acid (8.4 g, 0.05 mol) and 2,5-dibromothiophene **27** (6.48 g, 0.02 mol) in toluene (100 mL) was added a solution of Na_2CO_3 (10.6 g, 0.100 mol) in water (15 mL), and the mixture was purged with nitrogen for 15 min. Tetrakis(triphenylphosphine) palladium(0) (0.24 g, 0.20 mmol) was added, and the mixture was heated to 85 °C and stirred for 24 h. The solution was then cooled and poured into methanol (300 mL). The yellow precipitate was filtered and washed with water, 5% HCl solution, and again with water. The product was chromatographed on silica gel with hexane/methylene chloride (1:1 v/v) as the eluant to give a light-yellow powder of 2,5-bis[4-(methylthio)phenyl]thiophene (5.78 g, 88%), mp 218−220 °C. m/z (EI): 328 (M^+, 100%). ^{1}H NMR ($CDCl_3$): δ 7.54 (d, J = 8.4 Hz, 4 H), 7.27 (d, J = 8.4 Hz, 4 H), 7.24 (s, 2 H), 2.52 (s, 6 H) ppm. ^{13}C NMR ($CDCl_3$): δ 142.8, 137.8, 131.2, 126.9, 125.9, 123.7, 15.9 ppm. Anal. Calcd for $C_{18}H_{16}S_3$ (328.5 g/mol): C, 65.81; H, 4.91; S, 29.28. Found: C, 65.40; H, 4.66; S, 28.47. To a mixture of 2,5-bis[4-(methylthio)phenyl]-thiophene (3.28 g, 0.010 mol) and sodium *tert*-butylthiolate (3.36 g, 0.030 mol), dry dimethylformamide (DMF) (80 mL) was added with vigorous stirring, and the reaction mixture was refluxed for 6 h.[63] The solution was cooled to 20 °C and poured into 10% HCl (200 mL), and the precipitate was filtered off, washed with water and cold ethanol, and dried in vacuo to give dithiol **31a** (2.80 g, 93%), mp 216−217 °C. m/z (EI): 300 (M^+, 100%). ^{1}H NMR ($CDCl_3$): δ 7.49 (d, J = 8.5 Hz, 2 H), 7.29 (d, J = 8.5 Hz, 2 H), 7.23 (s, 2 H), 3.50 (s, 2 H).

Dithiol 32a was synthesized starting with 5,5′-dibromo-2,2′-bithiophene and using the same procedure as for **31a**. It was used directly for the next step.

Dithiol 33a was synthesized starting with 1,4-dibromobenzene using the same procedure as for **31a**. m/z (EI): 294 (M^+, 100%). ^{1}H NMR ($CDCl_3$): δ 7.62 (s, 4 H), 7.51 (d, J = 7.9 Hz, 4 H), 7.36 (d, J = 7.9 Hz, 4 H), 3.51 (s, 2 H) ppm. ^{13}C NMR ($CDCl_3$): δ 139.3, 138.1, 130.0, 129.8, 127.6, 127.2 ppm.

Dithiol 34a was synthesized starting with 4,4′-dibromobiphenyl using the same procedure as for **31a**. The crude product was sublimed in vacuo to give a light-yellow powder (yield, 51%), which is insoluble in common organic solvents, mp 380−385 °C. m/z (EI): 370 (M^+, 60%), 338 (M^+, 100%).

Dithioacetyl 31. Dithiol **31a** (2.50 g, 8.0 mmol) in dry chloroform (50 mL) was treated with acetyl chloride (1.33 g, 0.017 mol) and triethylamine (1.72 g, 0.017 mol), and the product was purified by flash column chromatography on silica gel with hexane/methylene chloride (1:1 v/v) as the eluant to give a light-yellow powder of compound **31** (2.71 g, 90%), mp 210−211 °C. m/z (EI): 384 (M^+, 100%). ^{1}H NMR ($CDCl_3$): δ 7.66 (d, J = 8.3 Hz, 2 H), 7.44 (d, J = 8.3 Hz, 2 H), 7.34 (s, 2 H), 2.45 (s, 6 H) ppm. ^{13}C NMR ($CDCl_3$): δ 193.9, 143.2, 135.2, 134.9, 127.0, 126.2, 125.0, 30.2 ppm. Anal. Calcd for $C_{20}H_{16}O_2S_3$ (384.5 g/mol): C, 62.47; H, 4.19; S, 25.02. Found: C, 62.75; H, 3.99; S, 24.73.

Dithioacetyl 32. This compound was synthesized using the same procedures as for compound **31**: yellow powder (yield, 76%), mp 248−249 °C. m/z (EI): 466 (M^+, 100%). ^{1}H NMR ($CDCl_3$): δ 7.61 (d, J = 8.2 Hz, 4 H), 7.40 (d, J = 8.2 Hz, 4 H), 7.26 (d, J = 3.7 Hz, 2 H), 7.17 (d, J = 3.7 Hz, 2 H), 2.43 (s, 6 H) ppm. ^{13}C NMR ($CDCl_3$): δ 137.3, 134.9, 134.7, 127.1, 126.1, 125.9, 124.9, 124.7, 123.1, 30.1 ppm.

Dithioacetyl 33. This compound was synthesized using the same procedures as for compound **31**: yellow powder (yield, 89%), mp 175−176 °C. m/z (EI): 378 (M^+, 100%). ^{1}H NMR ($CDCl_3$): δ 7.62 (s, 4 H), 7.51 (d, J = 7.9 Hz, 4 H), 7.36 (d, J = 7.9 Hz, 4 H), 3.51 (s, 2 H) ppm. ^{13}C NMR ($CDCl_3$): δ 194.2, 141.7, 139.5, 134.8, 127.8, 127.6, 126.9, 30.3 ppm.

Dithioacetyl 34. This compound was synthesized using the same procedures as for compound **31**: yellow powder (yield, 79%), mp 267 °C. m/z (EI): 454 (M^+, 100%). ^{1}H NMR ($CDCl_3$): 7.74 (d, J = 7.9 Hz, 4 H), 7.71−7.69 (m, 8 H), 7.51 (d, J = 7.9 Hz, 4 H), 2.46 (s, 6 H) ppm. ^{13}C NMR ($CDCl_3$): δ 194.1, 141.8, 139.9, 139.2, 134.8, 127.8, 127.6, 127.5, 126.9, 30.2 ppm. Anal. Calcd for $C_{28}H_{22}O_2S_2$ (454.5 g/mol): C, 73.40; H, 4.48; S, 13.69. Found: C, 73.98; H, 4.88; S, 14.11.

Monothioacetyl 35. This compound was prepared from bromobenzene and 4-(methylthio)phenylboronic acid using similar procedures as described for **31**: white solid (yield, 80%), mp 113−114 °C. m/z (EI): 228 (M^+, 70%), 186 (M^+, 100%). ^{1}H NMR ($CDCl_3$): δ 7.61 (m, 4 H), 7.43 (m, 4 H), 7.36 (d, J = 7.3 Hz, 1 H), 7.07 (m, 2H) 2.43 (s, 3H) ppm. ^{13}C NMR ($CDCl_3$): δ 193.8, 142.4, 140.2, 134.7, 128.8, 127.8, 127.7, 127.1, 126.9, 30.1 ppm.

Monothioacetyl 36. This compound was prepared from 4-bromobiphenyl and 4-(methylthio)benzeneboronic acid using similar procedures as described for **31**: white solid (yield, 73%), mp 204−205 °C. m/z (EI): 304 (M^+, 80%), 262 (M^+, 100%). ^{1}H NMR ($CDCl_3$): δ 7.66 (m, 6H), 7.46 (m, 6H), 7.34 (d, J = 7.3 Hz, 1H), 2.44 (s, 3H) ppm. ^{13}C NMR ($CDCl_3$): δ 193.8, 141.9, 140.6, 140.0, 138.9, 134.7, 132.5, 128.8, 127.7, 127.5, 127.3, 127.1, 126.9, 30.1 ppm. Anal. Calcd for $C_{20}H_{16}OS$ (304.4 g/mol): C, 78.91; H, 5.30; S, 10.53. Found: C, 78.99; H, 5.10; S, 10.78.

5-Methylthio-2,2′-bithiophene 37. To a solution of 2,2′-bithiophene (10.0 g, 0.062 mol) in diethyl ether (50 mL) was added *n*-BuLi (2.5 M solution in hexane, 26.4 mL, 0.066 mol) at 20 °C. The mixture was refluxed for 30 min and cooled to −78 °C, and sulfur powder (2.11 g, 0.066 mol) was added in one portion. The reaction mixture was stirred at −78 °C for 10 min and then gradually warmed to 20 °C and stirred for 15 min. It was then cooled to −78 °C, and methyl iodide (9.0 g, 0.066 mol) was added. The mixture was stirred at 20 °C overnight and then poured into water and extracted with diethyl ether (3 × 50 mL). The combined organic solution was washed with water and saturated NaCl solution and dried over $MgSO_4$. After removal of the solvent, the residue was distilled in vacuo to give compound **37** (10.3 g, 78%) as a colorless oil. m/z (EI): 212 (M^+, 100%). ^{1}H NMR ($CDCl_3$): δ 7.21 (dd, J = 5.1 Hz, 1.1 Hz, 1 H), 7.13 (dd, J = 3.6 Hz, 1.1 Hz, 1 H), 7.01−7.00 (m, 1 H), 7.00 (d, J = 5.1 Hz, 1 H), 6.98 (d, J = 3.6 Hz, 1 H), 2.50 (s, 3 H) ppm. ^{13}C NMR ($CDCl_3$): δ 139.6, 137.0, 136.2, 131.8, 127.8, 124.5, 123.8, 123.7, 22.1 ppm. Anal. Calcd for $C_9H_8S_3$ (212.4 g/mol): C, 50.90; H, 3.80; S, 45.36. Found: C, 51.02; H, 3.70; S, 44.41.

Dithioacetyl 38. To a solution of 4-methylthio-2,2′-bithiophene **37** (4.0 g, 0.019 mol) in THF (20 mL) was added *n*-BuLi (2.5 M solution in THF, 8 mL, 0.020 mol) at 20 °C, and the mixture was refluxed for 30 min. It was then cooled to 20 °C, CuCl (0.5 g, 5 mmol) was added, and the mixture was refluxed overnight. After quenching with 10% HCl, the mixture was extracted with toluene (60 mL), and the organic phase was separated and dried over $MgSO_4$. The solvent was removed in vacuo, and methanol was added to the residue. The resulting precipate was filtered off and washed subsequently with 10% HCl, water, methanol, and hexane to yield, after drying in vacuo, 5,5‴-bis(methylthio)-[2,2′,5′,2″,5″,2‴]-quaterthiophene (1.8 g, 47%), mp 247−250 °C. ^{1}H NMR ($CDCl_3$): δ 7.07−6.98 (m, 8 H), 2.52 (s, 6 H) ppm. ^{13}C NMR ($CDCl_3$): δ 139.0, 136.0, 135.9, 131.7, 124.6, 124.3, 124.2, 123.8, 22.0 ppm. To a mixture of the above 5,5‴-bis(methylthio)-[2,2′,5′,2″,5″,2‴]-quaterthiophene (0.54 g, 1.3 mmol) and sodium *tert*-butylthiolate (1.12 g, 10 mmol), dry DMF (10 mL) was added with vigorous stirring, and the reaction mixture was refluxed for 6 h. The solution was cooled and poured into 10% HCl solution (50 mL). The precipitate was filtered, subsequently washed with water and cold ethanol, and then dried in vacuo to give the crude product **38a** (0.46 g, 90%). ^{1}H NMR ($CDCl_3$): δ 7.12−7.02 (m, 8 H), 3.62 (s, 2 H) ppm. Protection with the acetyl group, as described for compound **5**, yielded compound **38** as a yellow powder (0.20 g, 35%), mp 225−226 °C. m/z (EI): 478 (M^+, 100%). ^{1}H NMR ($CDCl_3$): δ 7.15 (d, J = 3.8 Hz, 2 H), 7.11 (d, J = 3.8 Hz, 2 H), 7.10 (d, J = 3.8 Hz, 2 H), 7.07 (d, J = 3.8 Hz, 2 H), 2.44 (s, 6 H) ppm. ^{13}C NMR ($CDCl_3$): δ 194.0, 143.1, 136.5, 125.2, 124.6, 124.1, 123.4, 29.5 ppm. Anal. Calcd for $C_{20}H_{14}O_2S_6$ (478.7 g/mol): C, 50.18; H, 2.95. Found: C, 50.24; H, 2.87.

Acknowledgment. The authors thank their colleagues F. Wudl, N. Zhitenev, D. Abusch-Magder, A. de Picciotto, A. Erbe, H. E. Katz, E. A. Chandross, and E. Reichmanis for helpful discussions. Support from The Netherlands Organization for Scientific Research (NWO, TALENT fellowship) to B.d.B. is gratefully acknowledged. M.M.F. was supported by a fellowship within the Postdoc Program of the German Academic Exchange Service (DAAD). J.Z. is grateful for the support from P. Gregory Van Patten for an internship at Bell Laboratories/Lucent Technologies.

LA0341052